



Published in final edited form as:

Neuron. 2009 December 10; 64(5): 645–662. doi:10.1016/j.neuron.2009.10.017.

A cluster of cholinergic pre-motor interneurons modulates mouse locomotor activity

Laskaro Zagoraiou¹, Turgay Akay¹, James F Martin², Robert M Brownstone³, Thomas M Jessell¹, and Gareth B Miles⁴

Thomas M Jessell: tmj1@columbia.edu

¹Howard Hughes Medical Institute, Kavli Institute for Brain Science, Depts. of Neuroscience, and Biochemistry and Molecular Biophysics, Columbia University, New York, NY 10032

²Institute of Biosciences and Technology, Texas A&M System Health Science Center, Houston, Texas 77030

³Departments of Surgery, and Anatomy & Neurobiology, Neuroscience Institute, Dalhousie University, Halifax, Canada

⁴School of Biology, University of St Andrews, St Andrews, Fife, KY169TS, UK

Summary

Mammalian motor programs are controlled by networks of spinal interneurons that set the rhythm and intensity of motor neuron firing. Motor neurons have long been known to receive prominent ‘C-bouton’ cholinergic inputs from spinal interneurons, but the source and function of these synaptic inputs have remained obscure. We show here that the transcription factor Pitx2 marks a small cluster of spinal cholinergic interneurons, V_{0C} neurons, that represents the sole source of C-bouton inputs to motor neurons. The activity of these cholinergic interneurons is tightly phase-locked with motor neuron bursting during fictive locomotor activity, suggesting a role in the modulation of motor neuron firing frequency. Genetic inactivation of the output of these neurons impairs a locomotor task-dependent increase in motor neuron firing and muscle activation. Thus V_{0C} interneurons represent a defined class of spinal cholinergic interneurons with an intrinsic neuromodulatory role in the control of locomotor behavior.

Keywords

cholinergic interneurons; synapses; locomotor activity; neuromodulation

Introduction

Motor behaviors are constructed and constrained by neural circuits that coordinate the activation of skeletal muscles. The immediate task of regulating the limb muscles that control many aspects of vertebrate locomotor behavior has been assigned to circuits in the spinal cord, and in particular to networks of interneurons that determine the temporal dynamics of motor neuron activation. Elemental features of locomotion – the rhythm and pattern of motor neuron

Correspondence to: Thomas M Jessell, tmj1@columbia.edu.

Publisher's Disclaimer: This is a PDF file of an unedited manuscript that has been accepted for publication. As a service to our customers we are providing this early version of the manuscript. The manuscript will undergo copyediting, typesetting, and review of the resulting proof before it is published in its final citable form. Please note that during the production process errors may be discovered which could affect the content, and all legal disclaimers that apply to the journal pertain.

firing – are controlled by sets of excitatory and inhibitory interneurons that use fast-acting amino acid transmitters (Hochman and Schmidt, 1998; Cazalets et al., 1996; Shefchyk and Jordan, 1985; Fetcho et al., 2008; Orsal et al., 1986). Locomotor programs can also undergo adaptive changes in response to the biomechanical demands of particular motor tasks (Gillis and Biewener, 2001). These context-dependent features of locomotion involve moment-by-moment changes in the frequency of firing of spinal motor neurons, usually triggered by slower-acting modulatory networks of supraspinal and intraspinal origin (Jordan et al., 2008; Grillner 2006). Much has been learned about the organization and function of descending modulatory systems, but the identity, connectivity, and physiological roles of intrinsic spinal modulatory interneurons have been more difficult to untangle.

In many regions of the CNS, modulatory influences on neuronal output and behavior are mediated by sets of cholinergic interneurons that elicit a diverse array of post-synaptic responses. The activation of cortical cholinergic systems modulates sensory threshold, states of attention, and the consolidation of memory (Pauli and O'Reilly, 2008; Giocomo and Hasselmo, 2007; Lawrence, 2008). In subcortical regions, cholinergic interneurons regulate the output of dopaminergic pathways implicated in sensory-motor learning, action selection, and reward (Mena-Segovia et al., 2008; Joshua et al., 2008; Wang et al., 2006; Maskos et al., 2005). Many of these insights into cholinergic modulatory function have emerged through pharmacological manipulation of cholinergic receptor systems, although the widespread distribution of most receptors (Wess, 2003) has made it difficult to establish a clear link between the dynamics of cholinergic microcircuitry and physiological function (Wess, 2003). Defining the contribution of individual classes of cholinergic modulatory interneurons to specific behaviors has therefore been a challenge.

The spinal cord contains several classes of cholinergic interneurons with proposed roles in sensory processing and motor output (Barber et al., 1984; Phelps et al., 1984; Huang et al., 2000). The best characterized spinal cholinergic circuit involves a recurrent excitatory connection from motor neurons to Renshaw interneurons, mediated by the activation of nicotinic receptors (Willis, 1971; Alvarez and Fyffe, 2007). Motor neurons themselves also receive synaptic input from recurrent motor axon collaterals (Lagerback et al., 1981). But the most prominent cholinergic input to motor neurons takes the form of C-boutons, a set of large synaptic terminals that are concentrated on motor neuron cell bodies and proximal dendrites (Conradi and Skoglund, 1969; Nagy et al., 1993; Li et al., 1995). Cholinergic C-boutons align with post-synaptic m2 class muscarinic receptors and Kv2.1 class K⁺ channels (Hellstrom et al., 2003; Muennich and Fyffe, 2004; Wilson et al., 2004), suggesting that these synapses exert a modulatory influence on motor neuron firing (Brownstone et al., 1992). The activation of muscarinic receptors on spinal neurons reduces spike after-hyperpolarization and leads to a marked enhancement in the frequency of motor neuron firing (Miles et al., 2007). Conversely, blockade of muscarinic receptors in isolated spinal cord preparations decreases motor neuron output (Miles et al., 2007). Together, these findings have led to the idea that C-bouton synapses exert a modulatory influence on spinal motor output.

The neuronal source of C-bouton terminals has proved elusive. They do not derive from descending supraspinal axons (McLaughlin, 1972; VanderHorst and Ulfhake, 2006), or from motor axon collaterals (Hellstrom et al., 1999; Miles et al., 2007), and so by elimination, are thought to originate from one or more populations of spinal interneurons. The persistence of C-boutons after intraspinal lesions has led to the suggestion that they derive from cholinergic interneurons that are interspersed amongst motor neurons in the ventrolateral spinal cord (Hellstrom, 2004). Analysis of the activity-induced pattern of c-fos expression during locomotion, however, shows strong labeling of cholinergic interneurons adjacent to the central canal (Huang et al., 2000). Consistent with this, genetic lineage tracing in mice has provided evidence that C-boutons derive from one or more of cholinergic interneuron classes that

populate the intermediate zone of the spinal cord (Miles et al., 2007). But since there are no selective molecular markers for neurons that give rise to C-boutons, the circuitry and physiology of this intrinsic cholinergic system, and its contribution to mammalian motor behavior, have yet to be defined.

We set out to define discrete functional populations of interneurons in mouse spinal cord on the basis of their transcription factor profile, neurotransmitter phenotype, and connectivity. We show here that the paired-like homeodomain transcription factor *Pitx2* (Semina et al., 1996) defines a small set of cholinergic V0 interneurons positioned close to the central canal, and establish that these neurons represent the sole source of C-bouton synapses. The firing of cholinergic V0 interneurons is tightly phase-locked with motor neuron burst activity during fictive locomotor episodes, indicative of their recruitment during motor behavior. To explore the consequences of inactivating the output of these cholinergic interneurons we eliminated Choline Acetyl Transferase (ChAT), the sole synthetic enzyme for acetylcholine (ACh), from cholinergic V0 neurons. Mice in which cholinergic V0 neurons have been deprived of ChAT expression are impaired in their ability to increase the activation of specific muscles during certain locomotor behaviors, suggesting that recruitment of this set of cholinergic interneurons is required for the task-dependent enhancement of motor neuron firing. Together, our findings define the organization and properties of a discrete set of spinal cholinergic interneurons that exert a context-dependent modulatory influence on motor behavior.

Results

***Pitx2* is expressed by a small subset of V0 interneurons**

To define markers of discrete sets of spinal interneurons we performed a microarray screen with cDNA probes derived from dorsal and ventral domains of p8 mouse lumbar spinal cord (Figure S1A). We identified 82 genes with a ventral:dorsal enrichment ratio of 3.0 or greater, and used *in situ* hybridization histochemistry to determine the profile of expression of these genes. This analysis identified seven genes with patterns of expression that were confined to subsets of interneurons in intermediate and ventral spinal cord (Figure S1B-F). In this study we focus on the phenotype, organization, and function of interneurons defined by one of these genes, which encodes the paired-like homeodomain protein *Pitx2* (Semina et al., 1996).

In post-natal lumbar spinal cord, expression of *Pitx2* was confined to a longitudinally-arrayed cluster of cells positioned close to the central canal (Figure 1A, B). A similar profile of *Pitx2* expression was detected at thoracic and cervical levels, although at cervical levels the domain of *Pitx2*⁺ neurons extended slightly more laterally (Figure 1C, D). From the outset, *Pitx2* expression was restricted to a small group of neurons (Figure S2A-C). At lumbar levels, *Pitx2* expression was first detected at embryonic day (e) 11.5 to 12.0 (Figure S2C), and by late embryonic stages, was restricted to a small group of neurons in the intermediate domain, close to the central canal (Figure S2D). The expression of *Pitx2* by neurons in this medial column persisted until at least p30 (Figure S2E).

Pitx2⁺ neurons comprised two phenotypic subsets, one that co-expressed the cholinergic markers ChAT and vAChT (vesicular acetylcholine transporter), and a second that expressed the vesicular glutamate transporter *vGluT2* (Figure 1E-I"). Neurons in the peri-central canal region of p8 lumbar spinal cord did not co-express *vAChT* and *vGluT2* (Figure S3), indicating that these two neurotransmitter-defined sets represent distinct subpopulations. Cholinergic and glutamatergic *Pitx2*⁺ neurons were differentially distributed along the rostro-caudal axis of the lumbar spinal cord. At rostral lumbar levels, the majority of *Pitx2*⁺ neurons expressed cholinergic markers, whereas glutamatergic *Pitx2*⁺ neurons predominated at more caudal lumbar levels (Figure 1J). Cholinergic and glutamatergic *Pitx2*⁺ neurons were also detected at thoracic and cervical levels of the spinal cord (data not shown). Thus, *Pitx2* marks a small

subset of interneurons that can be further subdivided on the basis of neurotransmitter phenotype. *Pitx2* expression distinguishes this set of cholinergic interneurons from a nearby population of central canal cluster (C^3) neurons (Barber et al., 1984; Phelps et al., 1984) that also express cholinergic phenotype, but lack *Pitx2* expression (Figure S4).

We used genetic lineage tracing to determine the developmental origin of cholinergic and glutamatergic *Pitx2*⁺ neurons. The provenance of these interneurons was analyzed in a *Dbx1::nlsLacZ* transgenic line in which the post-mitotic perdurance of LacZ expression marks V0 interneurons (Pierani et al., 2001). In e12.5 *Dbx1::nlsLacZ* mice we found that ~80% of *Pitx2*⁺ neurons co-expressed LacZ (Figure 1L-M'), indicating that they correspond to V0 neurons. Analysis of *Dbx1* null mutant embryos, which lack V0 interneurons (Pierani et al., 2001), revealed an absence of *Pitx2* expression from neurons in the intermediate spinal cord (Figure 1N, O), confirming the V0 identity of *Pitx2*⁺ interneurons. This transcriptionally-defined population represents a very minor subset of the total V0 interneuron cohort: *Pitx2* was expressed by only 5% of all LacZ⁺ neurons in e12.5 *Dbx1::nlsLacZ* embryos (Figure 1K, L). V0 interneurons have been shown to comprise *Evx1/2*⁺ (V0_V) and *Evx1/2*⁻ (V0_D) divisions (Lanuza et al., 2004). Soon after their generation, virtually all *Pitx2*⁺ neurons co-expressed *Evx1*, albeit transiently (Figure 1P, Q). Thus, the cholinergic (V0_C) and glutamatergic (V0_G) interneuron populations marked by *Pitx2* appear to constitute small subsets of V0_V interneurons.

Genetic tracing of V0_C and V0_G interneuron connectivity

To define the connectivity of V0_C and V0_G neurons we crossed a mouse *Pitx2::Cre* line, which directs expression of Cre recombinase selectively in *Pitx2*⁺ neurons (Liu et al., 2003) with conditional *Thy1.lsl.YFP*, or *Tau.lsl.mGFP* reporter strains (Buffelli et al., 2003; Bareyre et al., 2005; Hippenmeyer et al., 2005). We detected fluorescent protein (FP) expression in a small subset of interneurons close to the central canal (Figure 2A, B). At rostral lumbar levels, FP expression was detected in 66% of all *Pitx2*⁺ neurons in *Thy1.lsl.YFP* mice, and in 74% of all *Pitx2*⁺ neurons in *Tau.lsl.mGFP* mice (Figure 2C-D' and data not shown). Examination of the neurotransmitter status of genetically marked neurons in *Tau.lsl.mGFP* mice revealed FP expression in 94% of cholinergic *Pitx2*⁺ interneurons, and in 56% of non-cholinergic *Pitx2*⁺ interneurons. Thus V0_C interneurons are labeled with high efficiency in *Tau.lsl.mGFP* mice.

To trace the targets of V0_C and V0_G neurons, we mapped FP-labeled axons and terminals in the spinal cord of *Pitx2::Cre; Tau.lsl.mGFP* mice, in conjunction with synaptic expression of the cholinergic markers vAChT and ChAT, and the glutamatergic marker vGluT2. Analysis of the overall pattern of FP-labeled axons and terminals from p8 to p25 revealed a high density in the ventral horn and intermediate zone, and a lower density in the dorsal horn (Figures 3A, S5). In the ventral horn, the cell bodies and proximal dendrites of virtually all vAChT⁺ motor neurons were studded with large FP-labeled boutons (Figure 3B, C) whereas more distal dendritic domains exhibited a > 20-fold lower FP⁺ bouton density (Figure 3H, I). We found that ~99% of the FP-labeled boutons on motor neurons expressed vAChT, and none of them co-expressed vGluT2 (Figure 3D-D'''). Conversely, 95% of all vAChT⁺ C-boutons on motor neurons expressed FP. Consistent with their identity as C-boutons, FP-labeled terminals on motor neurons were aligned with post-synaptic m2 muscarinic receptors and Kv2.1 channels (Figure 3F, G). These findings, taken together with the 94% labeling efficiency of cholinergic *Pitx2*⁺ interneuron cell bodies, indicate that V0_C neurons represent the sole source of C-boutons. Moreover, motor neurons receive preferential input from the V0_C subset of *Pitx2*⁺ neurons.

We next examined the connectivity of *Pitx2*⁺ neurons with spinal interneurons. We detected FP-labeled vGluT2⁺ boutons in the intermediate zone and dorsal horn of *Pitx2::Cre; FP* reporter mice (Figure 3E-E''; data not shown), providing evidence that the V0_G class of *Pitx2*⁺ neurons

forms connections with spinal interneurons. We also detected a low density of FP-labeled vAChT⁺ boutons in the intermediate zone of the spinal cord of p20 to p40 *Pitx2::Cre; Tau.lsl.mGFP* mice (data not shown), suggestive of synaptic contact with ventral interneurons. We therefore examined whether two classes of interneurons implicated in the regulation of motor neuron output, V2a interneurons (Peng et al., 2007; Al-Mosawie et al., 2007; Lundfald et al., 2007; Crone et al., 2008) and Renshaw cells (Alvarez and Fyffe, 2007), are contacted by V0_C neurons. The cell bodies and proximal dendrites of V2a neurons, defined by FP expression in *Sox14::eGFP* mice (Crone et al., 2008), were contacted only sparsely by vAChT⁺ boutons (< 4 boutons/neuron; 37 neurons) but by many vGluT1⁺ terminals (Figure 4A, B, C, D-D'', R; Al-Mosawie et al., 2007). The cell bodies and dendrites of calbindin⁺ Renshaw cells were contacted by many vAChT⁺ boutons (Figure 4A, E, F, R). But analysis of *Pitx2::Cre; Tau* or *Thy1* reporter mice revealed that none of them were FP-labeled (Figure 4E, F, 0/132 boutons; 8 neurons). Thus, Renshaw cells lack V0_C (or V0_G) input, although they receive cholinergic innervation from the axon collaterals of motor neurons (Figure 4G, H-H''). These findings argue for selectivity in the target connectivity of V0_C interneurons (Figure 4R). To assess whether *Pitx2*⁺ V0 neurons innervate ipsilateral and/or contralateral targets we identified interneurons after unilateral hindlimb muscle injection of pseudorabies PRV 614 (mRFP1) transneuronal tracer in p15 and p30 mice (Banfield et al., 2003; Smith et al., 2000; Lanuza et al., 2004). 48-68 h after virus injection, 69% of GFP-labeled *Pitx2*⁺ neurons were located ipsilateral to the side of muscle injection, (54/78 labeled neurons; Figure S6), indicating that many *Pitx2*⁺ V0 neurons project to ipsilateral motor neurons.

We also assessed the nature and origin of synaptic inputs to V0_C interneurons. In p24 *Pitx2::Cre; Thy1.lsl.YFP* mice, the cell bodies of vAChT⁺, FP-labeled V0_C neurons received many vGluT2⁺ bouton contacts (> 50 per neuron), an indication of excitatory input from glutamatergic interneurons and/or descending projections (Figure 4I-J, K-L). In contrast, we detected few vGluT1⁺ synaptic contacts (~10 boutons per neuron; Figure 4P-P'''), reflecting sparse sensory and/or corticospinal input (Betley et al., 2009). vAChT⁺, FP-labeled V0_C neurons also received many GAD67⁺ GABAergic inhibitory inputs (> 50 boutons per neuron) (Figure 4Q-Q'''). We also detected serotonergic contacts (> 20 per neuron) on the cell body and proximal dendrites of FP-labeled V0_C neurons (Figure 4M-O, R), presumably reflecting brainstem serotonergic input. Thus, V0_C neurons receive integrate input from glutamatergic, GABAergic, and monoaminergic pathways.

Coordination of V0_C neuron and motor neuron activity during locomotor episodes

We examined the physiological properties and functional connectivity of *Pitx2*⁺ V0 neurons using whole-cell patch clamp recordings from FP-labeled neurons in hemisectioned lumbar spinal cord preparations obtained from p4 to p8 *Pitx2::Cre; Thy1.lsl.YFP* mice (Figure 5A-D). FP-labeled neurons exhibited low whole-cell capacitance and moderate input resistance (~30 pF, ~450 MΩ, 16 neurons in control solution). At rest, 63% of FP-labeled neurons exhibited spontaneous activity, at low mean firing rates (3.1 ± 0.5 Hz, 10/16 neurons), with long action potentials (half-width = 2.81 ± 0.2 ms), and a prominent after-hyperpolarization (Figure 5E). Intracellular current injection enhanced firing rates to ~20 Hz, with little spike frequency adaptation (Figure 5F, G, H; 16 neurons). These features varied little amongst FP-labeled neurons, implying that V0_C and V0_G neurons share similar biophysical properties.

We next analyzed *Pitx2*⁺ V0 neuron firing frequency with motor neuron bursting during fictive locomotor activity. Whole-cell patch clamp recordings were obtained from FP-labeled neurons at rostral lumbar levels in hemisectioned spinal cord preparations exposed to a rhythmogenic drug cocktail (Figure 6A-C; Jiang et al., 1999). Most FP-labeled neurons (14/16 neurons) were tonically active (Figure 6A), and a few exhibited marked bursting activity (Figure 6C). The firing rate of tonically active FP-labeled neurons was modulated: ~80% of neurons fired more

rapidly in phase with motor burst activity in flexor associated L1-L3 ventral roots (Figure 6A; ~ 1.5 fold $>$ firing rate, $p < 0.01$ for 9/11 FP-labeled neurons). This phasic relationship was revealed most clearly when FP-labeled V0 neurons were hyperpolarized by current injection (-10pA to -100pA; Figure 6B). Under these conditions, $\sim 90\%$ of all FP-labeled neurons at L1 to L3 segments were phase-locked with motor neuron bursts recorded from flexor-associated L1-L3 ventral roots (Figure 6E, F, closed circles, 14/16 neurons). On occasion, rostrally-positioned V0 neurons also exhibited isolated inter-burst spikes (Figure 6C). Strikingly, these spikes coincided with transient excitatory activity recorded from L1-L3 ventral roots, as well as with brief periods of motor inactivity recorded from L5 motor roots (Fig. 6C, arrows). At L4 to L5 segments some FP-labeled V0 neurons fired maximally in phase with extensor-associated L4-L5 ventral root bursts (3 neurons), although others fired in phase with L1-L3 ventral root bursts (3 neurons; Figure 6F, open circles). The activity of Pitx2⁺ V0 neurons is therefore linked predominantly to the output of their segmentally aligned motor neuron targets, exclusively so at rostral lumbar levels.

Most Pitx2⁺ interneurons at rostral lumbar levels are cholinergic, suggesting that the phasic features of the general population of FP-labeled Pitx2⁺ V0 neurons are representative of the behavior of V0_C neurons. To define the properties of identified V0_C neurons, we analyzed mice in which V0_C neurons are marked selectively by crossing the *Pitx2::Cre* line with a *vAChT* FP reporter line (Figure 2E, F) (Experimental Procedures). At rostral lumbar levels, identified *vAChT* FP-labelled V0_C neurons also exhibited tonic activity with maximal firing in register with L1-L3 ventral root motor bursts (Figure 6D, F, open triangles, 4 neurons). The coordinated firing of Pitx2⁺ excitatory V0 neurons and motor neurons raises the possibility that these interneurons regulate ipsilateral motor output during locomotor activity.

To explore the basis of the phasic activity of Pitx2⁺ V0 interneurons we first assessed whether these neurons display intrinsic oscillatory properties. Whole-cell patch clamp recordings were made from FP-labeled neurons in transverse spinal cord slices obtained from p12-p13 *Pitx2::Cre; Tau.lsl.mGFP* mice. FP-labeled neurons were spontaneously active and the application of a rhythmogenic drug cocktail increased the firing rate of FP-labeled neurons, but oscillatory activity was not observed (Figure 5I, J; 6 neurons), suggesting that they lack intrinsic rhythmogenic properties.

To assess the origin of inputs responsible for the phasic activity of Pitx2⁺ V0 interneurons we recorded from FP-labeled neurons in L1 to L3 segments in hemisectioned spinal preparations. Antidromic activation of motor neurons by ventral root stimulation did not elicit synaptic responses in FP-labeled V0 neurons (4 neurons; data not shown), arguing against input from a recurrent excitatory pathway (Machacek and Hochman, 2006). Voltage clamp analysis of FP-labeled neurons during locomotor activity revealed barrages of excitatory postsynaptic current (EPSCs) in phase with ventral root bursts (Figure 7A, B; 13 *Thy1* FP-labeled neurons; 4 *vAChT* FP-labeled neurons). In contrast, IPSCs were detected during all phases of the motor burst cycle (Figure 7C, 7 *Thy1* FP-labeled neurons). Together, these findings support the idea that the bursting activity of Pitx2⁺ V0 neurons is driven by rhythmic excitatory input from spinal interneurons.

We also asked whether Pitx2⁺ V0 interneurons can be activated by sensory afferent input. Recordings from FP-labeled neurons during stimulation of segmentally-aligned dorsal roots (threshold 10 to 40 μ A) revealed sensory-evoked EPSCs (Figure 7D). Their latency (14.1 ± 1.0 ms, 7 *Thy1* FP-labeled neurons), variable onset (high 'jitter', coefficient of variation = 0.18) is indicative of indirect rather than monosynaptic excitatory input. Together, these physiological studies in isolated spinal cord preparations indicate that the phasic activity of Pitx2⁺ V0 interneurons is driven primarily by input from local excitatory interneurons.

A motor behavioral defect in mice lacking V0_C cholinergic output

To explore the contribution of V0_C interneurons to locomotor behavior we sought a means of inactivating the output of this set of neurons, while preserving the function of other classes of V0 neurons. Cre-mediated deletion of coding exons of the mouse *ChAT* gene generates a truncated, enzymatically inactive protein and effectively prevents cholinergic transmission by spinal neurons (Misgeld et al., 2002; Buffelli et al., 2003). We used this strategy to generate a V0 neuron-specific disruption in the gene encoding ChAT.

We compared the efficacy of ChAT elimination from V0_C neurons in mice in which *Pitx2::Cre* and *Dbx1::Cre* (Bielle et al., 2005) driver lines were crossed with a floxed *ChAT* (*ChAT^{fl/fl}*) allele (Buffelli et al., 2003). In *Pitx2::Cre; ChAT^{fl/fl}* mice analyzed between p0 and p30, ChAT expression was eliminated from ~55% of vAChT⁺ C-boutons (data not shown). In contrast, *Dbx1::Cre; ChAT^{fl/fl}* mice resulted in a virtually complete (> 99%, n = 503 boutons) loss of vAChT⁺, ChAT⁺ C-boutons (Figure 8A-F''). The depletion of ChAT in *Dbx1::Cre; ChAT^{fl/fl}* mice was selective, in that motor neurons still expressed ChAT (Figure 8A, D). C³ neurons can be labeled by *Dbx1::Cre* lineage tracing (Miles et al., 2007) (Figure S4), but C-bouton synapses with motor neurons derive exclusively from V0_C neurons. Moreover, the axonal projections of C³ neurons appear confined to the vicinity of the central canal (Barber et al., 1984; Phelps et al., 1984). Thus, C³ neurons do not exert a direct influence on motor output. We therefore analyzed the impact of eliminating V0_C output on locomotor behavior using *Dbx1::Cre; ChAT^{fl/fl}* mice.

Dbx1::Cre; ChAT^{fl/fl} mice exhibited an overtly normal developmental program and survived until adulthood (data not shown). Despite the loss of synaptic ChAT expression, the number of vAChT⁺ C-boutons in contact with the cell body and proximal dendrites of lumbar motor neurons was similar in *Dbx1::Cre; ChAT^{fl/fl}*, *Dbx1::Cre; ChAT^{fl/+}*, and wild type mice (Figure 8A, D; data not shown). The loss of ChAT expression from C-boutons was not accompanied by expression of the glutamatergic markers vGluT1 or vGluT2 (Figure 8G-H''). These vAChT⁺, ChAT-depleted C-boutons were still aligned with m2 muscarinic receptors and Kv2.1 class K⁺ channels (Figure 8I-J''), indicating that the post-synaptic organization of these synapses is preserved. Thus, ChAT-deficient V0_C neurons form structurally differentiated, albeit acetylcholine synthesis-deficient, synapses with motor neurons.

To examine the contribution of V0_C neurons to motor output, we focused on locomotor behavioral assays that uncover task-dependent modulation in the activation of limb muscles. In rodents walking and swimming elicit markedly different degrees of hindlimb muscle activation (Roy et al., 1985; de Leon et al., 1994) – the amplitude of gastrocnemius (Gs) electromyographic (EMG) activity, for instance, is greater during swimming than walking (Hutchison et al., 1989). We therefore monitored the degree of Gs muscle activation in mice subjected sequentially to walking and swimming.

To measure muscle activation, the Gs muscles of wild type (n = 8), *ChAT^{fl/fl}* (n = 14) and *Dbx1::Cre; ChAT^{fl/fl}* (n = 12) mice (p45 or older) were implanted with EMG recording electrodes (Pearson et al., 2005; Akay et al., 2006). Electrodes were also placed in the left and right tibialis anterior (TA) ankle flexor and Iliopsoas (Ip) hip flexor muscles as indicators of the overall fidelity of locomotor pattern. We detected no consistent differences in EMG patterns of control and *Dbx1::Cre; ChAT^{fl/fl}* mice during locomotor behavior. A clear alternation of Gs, compared to TA and Ip muscle activity, was evident during walking (Figure 9A, B). The normal alternation in the activity of left and right TA muscles was also preserved in *Dbx1::Cre; ChAT^{fl/fl}* mutant mice (Figure 9A, B). Thus, loss of V0_C neuronal output does not perturb locomotor pattern.

We next examined muscle activity in wild type mice during walking and swimming. The amplitude of the Gs muscle burst in control mice subjected to a swimming task was consistently larger than the burst observed when the same animals were walking (Figure 10A). The amplitude of TA muscle bursts was only marginally greater during swimming than walking, however (Figure 10A). We quantified the change in muscle activity during swimming and walking by monitoring the ratio of peak swim:walk (S:W) EMG amplitudes, revealing S:W ratios of 5.5 for the Gs muscle and 1.3 for the TA muscle (Figure 10B, D).

In *Dbx1::Cre; ChAT^{fl/fl}* mice subjected sequentially to walking and swimming tasks we observed that the enhancement of Gs burst amplitude during swimming was significantly diminished (S:W ratio of 3.5, $p < 0.01$) (Figure 10C) when compared to control littermates (Figure 10B). In contrast, the TA muscle S:W ratio was not significantly different between *Dbx1::Cre; ChAT^{fl/fl}* and control mice (Figure 10D). These EMG findings, in conjunction with physiological analyses, provide evidence that this locomotor task-dependent modulation of hindlimb muscle activity involves a $V0_C$ interneuron-mediated enhancement of motor neuron firing.

Discussion

Motor circuits in the spinal cord are the final neural arbiters of movement. The force and duration of muscle contraction is determined by the pattern of motor neuron firing which, in turn, reflects the coordinated activity of spinal interneurons. Pre-motor interneurons provide excitatory and inhibitory commands, and in addition are thought to modulate motor output during locomotor tasks. The identity, circuitry and behavioral contributions of such modulatory neurons have, however, been difficult to decipher. Our analysis of $V0_C$ neuronal circuitry and physiology suggests that this small cluster of cholinergic pre-motor interneurons exerts a modulatory influence on locomotor behavior, providing an initial insight into the function of an intrinsic spinal modulatory system.

Identity and diversity within the $V0$ interneuron cohort

Classical anatomical and physiological studies have provided evidence that spinal circuits dedicated to the control of motor output are constructed from a complex array of interneuron subtypes (Jankowska, 2001; Bannatyne et al., 2009). Most of these neurons derive from the four cardinal progenitor domains that subdivide the ventral half of the embryonic spinal cord (Jessell, 2000; Goulding, 2009), implying that a single progenitor domain gives rise to multiple interneuron subclasses. The $p0$ progenitor domain has been shown to give rise to two major groups of commissural inhibitory interneurons, $V0_V$ and $V0_D$ neurons (Pierani et al., 2001; Moran-Rivard et al., 2001; Lanuza et al., 2004). Our findings show that the $V0_V$ population can be further divided, in that it includes a small set of excitatory interneurons defined by the paired domain transcription factor *Pitx2*. And even this small *Pitx2*⁺ neuronal subset can be fractionated into discrete $V0_C$ cholinergic and $V0_G$ glutamatergic populations. The program for specification of $V0$ interneuronal subtype identity therefore assigns discrete molecular identities to neuronal subsets that comprise only a few percent of the cardinal $V0$ cohort.

Equivalent diversification of other cardinal interneuron domains would imply the existence of over a hundred molecularly distinct ventral interneuron subtypes – a variety far greater than revealed by physiological or anatomical classification schemes. Nevertheless, there is precedent for the idea that an individual ventral progenitor domain can give rise to molecularly and functionally diverse neuronal subclasses. Renshaw interneurons are known to represent only ~10% of the total $V1$ interneuron population (Sapir et al., 2004; Alvarez et al., 2005), and *Hb9*⁺ interneurons constitute an even smaller fraction of their cardinal interneuron class (Wilson et al., 2005). In addition, a dozen or more motor neuron subtypes derive from a single

progenitor domain (Dasen et al., 2005), with individual motor pools often comprising only ~5% of total segmental motor neuron number (McHanwell and Biscoe, 1981).

By analogy with the mechanisms that direct motor neuron columnar and pool identity (Dasen et al., 2005; Dasen and Jessell, 2009) the specification of Pitx2⁺ neurons within the V0 cohort could be initiated by a cell-intrinsic program of Hox protein repression. Notch signaling has been shown to direct binary differentiation of the cardinal V2 interneuron group into distinct glutamatergic V2a and GABAergic V2b subsets (Peng et al., 2007), and also contributes to neuronal diversification in the dorsal spinal cord (Mizuguchi et al., 2006). By extension, Notch signaling could drive the generation of discrete cholinergic and glutamatergic subtypes within the Pitx2⁺ V0 interneuron group. Thus, sequential ‘winner-take-all’ strategies of neuronal specification, initially a cell-intrinsic program of mutual Hox repression, and subsequently an intercellular program of Notch signaling, could underlie the progressive specification of neurons within the cardinal V0 population to a minority cholinergic V0_C fate.

The analysis of Pitx2⁺ V0 interneurons also reveals the extent of diversity in neurotransmitter phenotype and projection pattern that can emerge in the neuronal progeny of a single ventral progenitor domain. Most V0 interneurons exhibit GABAergic and/or glycinergic inhibitory character (Pierani et al., 2001; Lanuza et al., 2004; Moran-Rivard et al., 2001), but Pitx2⁺ V0_V interneurons are excitatory and use acetylcholine or glutamate as transmitters. Thus, a single ventral interneuron progenitor domain can give rise to interneurons of at least four different neurotransmitter phenotypes. Moreover many Pitx2⁺ V0 interneurons appear to send axons ipsilaterally, whereas inhibitory V0 interneurons project their axons across the midline to innervate contralateral motor neurons (Pierani et al., 2001). Thus progenitor provenance does not necessarily restrict the neurotransmitter phenotype or projection pattern of ventral interneurons.

Our findings also provide an insight into the contribution of neurotransmitter synthesis to the formation and maturation of interneuronal connections in mammalian CNS circuits. Selective elimination of ChAT from V0_C neurons has no obvious influence on the maturation and organization of C-bouton synapses with motor neurons. Similarly, elimination of ChAT from developing motor neurons and retinal amacrine neurons has no obvious anatomical impact on their development (Stacy et al., 2005; Myers et al., 2005). In contrast, glutamic acid decarboxylase (GAD) dependent synthesis and release of GABA appears to have a crucial role in the maturation of axonal arbors and synapses of GABAergic interneuron in visual cortex (Chattopadhyaya et al., 2007; Fagioloni and Hensch, 2000). The contribution of neurotransmitters to synaptic maturation in mammalian CNS circuits therefore differs as a function of neuronal subtype and transmitter status.

The circuitry and physiology of V0_C interneurons

V0_C neurons are the sole source of C-bouton synapses on spinal motor neurons. Their biophysical properties – slow tonic firing rates, broad action potentials and large after-hyperpolarizing potentials – are typical of cholinergic and monoaminergic modulatory neurons in other regions of the mammalian CNS (Masuko et al., 1986; Li and Bayliss, 1998; Bennett et al., 2000). The organization of V0_C neuronal projections is also suggestive of a modulatory role. In the lumbar spinal cord we estimate that motor neurons typically receive 80-100 C-bouton contacts, and motor neurons outnumber V0_C interneurons by a factor of ~10:1. Thus individual V0_C neurons are likely to contribute ~1000 cholinergic synaptic contacts with target motor neurons, a divergence that places them in a pivotal position to modulate motor output.

During locomotor episodes, V0_C neurons exhibit a rhythmic firing pattern that is tightly phase-locked to the activity of segmentally-aligned motor neuron targets. Other studies have revealed considerably greater variability in the relative firing phases of broad populations of ventral

glutamatergic interneurons (Butt et al., 2003, 2005). This presumably reflects the fact that this heterogeneous neuronal group is comprised both of last-order neurons that fire in register with motor bursts, and upstream locomotor network interneurons that would not necessarily exhibit such tight linkage (McCrea and Rybak, 2008; Brownstone and Wilson, 2008). One small population of glutamatergic interneurons, defined by Hb9 expression (Wilson et al., 2005), fires in phase with segmental motor output (Hinckley et al., 2005), but its contributions to locomotor function are still unclear (Brownstone and Wilson, 2008; Kwan et al., 2009).

V_{0C} neurons are unlikely to provide the major excitatory drive for motor neuron bursting. Rhythmic activity is maintained when V₀ cholinergic output is eliminated *in vivo*, and after blockade of muscarinic m2 receptors *in vitro* (Miles et al., 2007). More likely, the coordinated firing of V_{0c} neurons and motor neurons reflects common rhythmic input from components of the core locomotor network. In support of this view, physiological analysis shows that rhythmic variation in the frequency of excitatory synaptic input to V_{0C} interneurons coincides with activity in their aligned motor neuron targets. The spiking of V_{0C} interneurons also matches the burst activity of segmentally aligned motor neurons, and the cessation of activity in more caudally-located ‘antagonist’ motor neurons. We have not resolved whether individual V_{0C} neurons innervate motor neurons in an indiscriminate manner or whether they respect flexor-extensor, or pool-specific motor neuron characters. Nevertheless, our behavioral findings imply that descending or sensory pathways can activate spinal V_{0C} neuronal circuits in a manner that enhances the firing rate of motor pools in a task-appropriate manner. We note that V_{0C} neurons exhibit characteristics of ‘intrinsic’ modulatory interneurons (Katz, 1995).

The physiology and connectivity of V_{0C} neurons therefore suggests that they participate in spinal pre-motor circuits devoted to the modulation of motor output. Cholinergic signaling has previously been implicated in the generation of spinal motor rhythm (Cattaert et al., 1995; Quinlan et al., 2004; Cowley and Schmidt, 1994; Roberts et al., 2008; Hanson and Landmesser, 2003), although our findings imply that these activities are independent of V_{0C} neurons. At embryonic stages, cholinergic influences on locomotor rhythm are mediated by the recurrent collaterals of motor neurons themselves (Myers et al., 2005). Thus spinal cholinergic neurons involved in the generation of locomotor rhythm appear distinct from those involved in its modulation.

V_{0c} interneurons as modulators of locomotor behavior

Locomotion in terrestrial vertebrates depends on the ability of neural circuits to regulate the function of individual limb muscles in a dynamic fashion during different locomotor tasks, even over the course of a single stride (Gillis and Biewener, 2001). Our findings provide genetic, physiological and behavioral evidence for a task-dependent role for cholinergic V_{0C} neurons in the modulation of mouse locomotor behavior – genetic manipulations that remove cholinergic C-bouton signaling result in a significant impairment in the activation of the Gs muscle during swimming.

The demands of individual motor tasks – the transition from walking to swimming in our analysis – are likely to be transmitted to V_{0C} interneurons via sensory or descending systems (Figure 11). Once activated, ACh release from the C-bouton terminals of V_{0C} neurons is likely to engage m2 muscarinic receptors on motor neurons, reducing spike after-hyperpolarization and enhancing motor neuron firing frequency (Miles et al., 2007). The impairment of Gs muscle activation observed after elimination of V_{0C} neuronal output can therefore be explained by a failure to activate m2 muscarinic receptors at C-bouton synapses. Nevertheless, the reduction in Gs muscle activation in V₀ ChAT-depleted mice is incomplete. This could reflect the contribution of other modulatory systems that normally contribute to the regulation of motor neuron firing rate (Liu et al., 2009; Krieger et al., 1998), or a compensatory change in the

function of spinal networks after elimination of $V0_C$ cholinergic output (Myers et al., 2005, Stacy et al., 2005).

In the brain, cholinergic neurons have key roles in the attentional modulation of sensory processing streams (Giocomo and Hasselmo, 2007). In the owl optic tectum, the enhancement of neuronal responses to attended auditory and visual stimuli is mediated by cholinergic input from midbrain nuclei (Winkowski and Knudsen, 2008). In primate visual cortex, neuronal responses to images presented within attended receptive fields are elevated by activation of muscarinic signaling, and reduced by muscarinic antagonists (Herrero et al., 2008). In one sense, the role of the spinal $V0_C$ cholinergic interneuron system in the task-appropriate gain control of selected motor neuron groups can be considered a motor attentional counterpart to these supraspinal cholinergic influences on sensory processing. Further analysis of the organization and function of $V0_C$ interneurons may therefore provide more general insight into the role of cholinergic modulatory systems throughout the mammalian CNS.

Experimental Procedures

Differential Expression Screen

RNA was isolated from ventral and dorsal spinal cord tissue ($n = 3$ or 4 p8 mice for each sample) (Figure S1A) using the RNeasy Mini Kit (Qiagen), and aRNA was synthesized with Ambion's MessageAmp™ aRNA Kit (Catalog # 1750) and Biotin 11-CTP and Biotin 16-UTP (Enzo). Affymetrix Gene chip Mouse Genome 430 2.0 Arrays were hybridized, and results analyzed with the Gene Traffic software.

Generation of *Sox14::eGFP* and *vAChT::Isl::eGFP* mice

The *Sox14::eGFP* and *vAChT::Isl::eGFP* (*Isl::loxP-stop-loxP* cassette) targeting vectors (details in Supplemental Experimental Procedures) were electroporated into mouse ES cells (129sv/ev) selected with G418, and homologous recombinants identified by Southern blot analysis. Targeted mouse ES cells were microinjected into blastocysts and chimeric mice were crossed to C57BL/6J females. Additional mouse strains (Figure S8): *Dbx1::nlsLacZ* (Pierani et al., 2001), *Dbx1::Cre* (Bielle et al., 2005), *Pitx2::Cre* (*Pitx2^{Δabc}creneo*; Liu et al., 2003), *Thy1::Isl::YFP* (line15) (Buffelli et al., 2003; Bareyre et al., 2005), *Tau::Isl::mGFP-IRES-NLS-LacZ-pA* (Hippenmeyer et al., 2005), *Hb9::eGFP* (Wichterle et al., 2002), *ChAT^{fl/fl}* (Misgeld et al., 2002, Buffelli et al., 2003).

Histochemistry

In situ hybridization histochemistry was performed on 15-20 μ m cryostat sections as described (Dasen et al., 2005). Combined fluorescent *in situ* hybridization histochemistry/immunohistochemistry was performed on 15-20 μ m cryostat sections.

Immunohistochemistry

Immunohistochemistry was performed as described (<http://sklad.cumc.columbia.edu/jessell/resources/protocols.php>) (Betley et al., 2009). *Pitx2* antisera were generated in rabbit using the peptide MVPSAVTGVPGSSLC. Additional antibodies listed in Supplemental Experimental Procedures. Images were acquired on BioRad MRC 1024 or Zeiss LSM510 Meta confocal microscopes.

In vitro electrophysiology

Methods for recording from isolated spinal cord preparations have been described (Jiang et al., 1999). Further details provided in Supplemental Methods. Data are reported as mean \pm S.E. Differences in means were compared using Student's t-test. For analyses of interneuron firing

phases, the phasing of individual action potentials was normalized to the onset of rostral lumbar ventral root activity and circular plots generated where mean vector (arrow) direction represents the preferred firing phase and mean vector length (r) represents the concentration of action potentials around the mean (Butt et al., 2002). Relationships between preferred firing phases and ventral root activity were assessed using Rayleigh's test for uniformity (Kjaerulff and Kiehn, 1996; statistiXL software, Nedlands, WA, Australia). Values of $p < 0.05$ were considered significant.

Motor behavioral analysis

Adult mice were implanted with bipolar EMG recording electrodes (Pearson et al., 2005; Akay et al., 2006). EMG activities were recorded during free walking for ~20 min in a 78cm × 4cm Plexiglas runway. After walking trials, mice were placed in a tank with ~23°C water for ~2 min and EMG activity collected using Power1401 and Spike 2 (version 6.02, CED, Cambridge, UK) software, and analyzed by Spike 2, Excel 2003, and statistiXL (version 1.8). Data are reported as mean ± S.D. and differences in distributions were tested by using the Student's t-test (statistiXL). Values of $p < 0.05$ were considered significant.

Supplementary Material

Refer to Web version on PubMed Central for supplementary material.

Acknowledgments

We are grateful to Staceyann Doobar, Elizabeth Hwang, Qiaolian Liu and Natasha Permaul for technical assistance; Barbara Han, Monica Mendelsohn, Jennifer Kirkland and Susan Kales for help in the generation and upkeep of mice, and Susan Morton for antibody generation. We thank Lieven van der Veken for pseudorabies virus tracing, Silvia Arber for the *Tau.lsl.mGFP* line, Joshua Sanes for the *ChAT^{fl/fl}* line, Alessandra Pierani for advice on *Dbx1::Cre* mice, Tord Hjalt for an aliquot of anti-Pitx2 antibody, and Apostolos Klinakis for DNA constructs. Frederic Bretzner, Christopher Henderson, John Martin, Joriene de Nooij, Sebastian Poliak, Victor Rafuse and Keith Sillar provided helpful comments on the manuscript. L.Z. was supported by a Helen Hay Whitney Foundation Fellowship. TA is an HHMI research specialist. RMB is supported by grants from ProjectALS and the Canadian Institutes of Health Research. GBM is supported by grants from BBSRC UK, Project A.L.S., and Medical Research Scotland. JFM is supported by NIH grants R01 DE/HD12324 and DE16329. TMJ is supported by grants from Project ALS, The Harold and Leila Mathers Foundation, The Wellcome Trust, NIH RO1 NS33245, and is an HHMI Investigator.

References

- Akay T, Acharya HJ, Fouad K, Pearson KG. Behavioral and electromyographic characterization of mice lacking EphA4 receptors. *J Neurophysiol* 2006;96:642–651. [PubMed: 16641385]
- Al-Mosawie A, Wilson JM, Brownstone RM. Heterogeneity of V2-derived interneurons in the adult mouse spinal cord. *Eur J Neurosci* 2007;26:3003–3015. [PubMed: 18028108]
- Alvarez FJ, Fyffe RE. The continuing case for the Renshaw cell. *J Physiol* 2007;584:31–45. [PubMed: 17640932]
- Alvarez FJ, Jonas PC, Sapir T, Hartley R, Berrocal MC, Geiman EJ, Todd AJ, Goulding M. Postnatal phenotype and localization of spinal cord V1 derived interneurons. *J Comp Neurol* 2005;493:177–192. [PubMed: 16255029]
- Banfield BW, Kaufman JD, Randall JA, Pickard GE. Development of pseudorabies virus strains expressing red fluorescent proteins: new tools for multisynaptic labeling applications. *J Virol* 2003;77:10106–10112. [PubMed: 12941921]
- Bannatyne BA, Liu TT, Hammar I, Stecina K, Jankowska E, Maxwell DJ. Excitatory and inhibitory intermediate zone interneurons in pathways from feline group I and II afferents: differences in axonal projections and input. *J Physiol* 2009;587:379–399. [PubMed: 19047211]
- Barber RP, Phelps PE, Houser CR, Crawford GD, Salvaterra PM, Vaughn JE. The morphology and distribution of neurons containing choline acetyltransferase in the adult rat spinal cord: an immunocytochemical study. *J Comp Neurol* 1984;229:329–346. [PubMed: 6389613]

- Bareyre FM, Kerschensteiner M, Misgeld T, Sanes JR. Transgenic labeling of the corticospinal tract for monitoring axonal responses to spinal cord injury. *Nat Med* 2005;11:1355–1360. [PubMed: 16286922]
- Bennett BD, Callaway JC, Wilson CJ. Intrinsic membrane properties underlying spontaneous tonic firing in neostriatal cholinergic interneurons. *J Neurosci* 2000;20:8493–8503. [PubMed: 11069957]
- Betley JN, Wright CVE, Kawaguchi Y, Erdélyi F, Szabó G, Jessell TM, Kaltschmidt JA. Stringent specificity in the construction of a GABAergic presynaptic inhibitory circuit. *Cell* 2009;139:161–174. [PubMed: 19804761]
- Bielle F, Griveau A, Narboux-Neme N, Vigneau S, Sigrist M, Arber S, Wassef M, Pierani A. Multiple origins of Cajal-Retzius cells at the borders of the developing pallium. *Nat Neurosci* 2005;8:1002–1012. [PubMed: 16041369]
- Brownstone RM, Jordan LM, Kriellaars DJ, Noga BR, Shefchyk SJ. On the regulation of repetitive firing in lumbar motoneurons during fictive locomotion in the cat. *Exp Brain Res* 1992;90:441–455. [PubMed: 1426105]
- Brownstone RM, Wilson JM. Strategies for delineating spinal locomotor rhythm-generating networks and the possible role of Hb9 interneurons in rhythmogenesis. *Brain Res Rev* 2008;57:64–76. [PubMed: 17905441]
- Buffelli M, Burgess RW, Feng G, Lobe CG, Lichtman JW, Sanes JR. Genetic evidence that relative synaptic efficacy biases the outcome of synaptic competition. *Nature* 2003;424:430–434. [PubMed: 12879071]
- Butt SJ, Harris-Warrick RM, Kiehn O. Firing properties of identified interneuron populations in the mammalian hindlimb central pattern generator. *J Neurosci* 2002;22:9961–9971. [PubMed: 12427853]
- Butt SJ, Kiehn O. Functional identification of interneurons responsible for left-right coordination of hindlimbs in mammals. *Neuron* 2003;38:953–963. [PubMed: 12818180]
- Butt SJ, Lundfald L, Kiehn O. EphA4 defines a class of excitatory locomotor-related interneurons. *Proc Natl Acad Sci USA* 2005;102:14098–14103. [PubMed: 16172411]
- Cattaert D, Pearlstein E, Clarac F. Cholinergic control of the walking network in the crayfish *Procambarus clarkii*. *J Physiol Paris* 1995;89:209–220. [PubMed: 8861819]
- Cazalets JR, Borde M, Clarac F. The synaptic drive from the spinal locomotor network to motoneurons in the newborn rat. *J Neurosci* 1996;16:298–306. [PubMed: 8613795]
- Chattopadhyaya B, Di Cristo G, Wu CZ, Knott G, Kuhlman S, Fu Y, Palmiter RD, Huang ZJ. GAD67-mediated GABA synthesis and signaling regulate inhibitory synaptic innervation in the visual cortex. *Neuron* 2007;54:889–903. [PubMed: 17582330]
- Conradi S, Skoglund S. Observations on the ultrastructure and distribution of neuronal and glial elements on the motoneuron surface in the lumbosacral spinal cord of the cat during postnatal development. *Acta Physiol Scand Suppl* 1969;333:5–52. [PubMed: 5386538]
- Cowley KC, Schmidt BJ. A comparison of motor patterns induced by N-methyl-D-aspartate, acetylcholine and serotonin in the in vitro neonatal rat spinal cord. *Neurosci Lett* 1994;171:147–150. [PubMed: 8084477]
- Crone SA, Quinlan KA, Zagoraïou L, Droho S, Restrepo CE, Lundfald L, Endo T, Setlak J, Jessell TM, Kiehn O, Sharma K. Genetic ablation of V2a ipsilateral interneurons disrupts left-right locomotor coordination in mammalian spinal cord. *Neuron* 2008;60:70–83. [PubMed: 18940589]
- Dasen JS, Jessell TM. Hox networks and the origins of motor neuron diversity. *Curr Top Dev Biol* 2009;88:1–32. [PubMed: 19651300]
- Dasen JS, Tice BC, Brenner-Morton S, Jessell TM. A Hox regulatory network establishes motor neuron pool identity and target-muscle connectivity. *Cell* 2005;123:477–491. [PubMed: 16269338]
- de Leon R, Hodgson JA, Roy RR, Edgerton VR. Extensor- and flexor-like modulation within motor pools of the rat hindlimb during treadmill locomotion and swimming. *Brain Res* 1994;654:241–250. [PubMed: 7987674]
- Fagiolini M, Hensch TK. Inhibitory threshold for critical-period activation in primary visual cortex. *Nature* 2000;404:183–186. [PubMed: 10724170]
- Fetcho JR, Higashijima S, McLean DL. Zebrafish and motor control over the last decade. *Brain Res Rev* 2008;57:86–93. [PubMed: 17825423]

- Gillis GB, Biewener AA. Hindlimb muscle function in relation to speed and gait: in vivo patterns of strain and activation in a hip and knee extensor of the rat (*Rattus norvegicus*). *J Exp Biol* 2001;204:2717–2731. [PubMed: 11533122]
- Giocomo LM, Hasselmo ME. Neuromodulation by glutamate and acetylcholine can change circuit dynamics by regulating the relative influence of afferent input and excitatory feedback. *Mol Neurobiol* 2007;36:184–200. [PubMed: 17952661]
- Goulding M. Circuits controlling vertebrate locomotion: moving in a new direction. *Nat Rev Neurosci* 2009;10:507–518. [PubMed: 19543221]
- Grillner S. Biological pattern generation: the cellular and computational logic of networks in motion. *Neuron* 2006;52:751–766. [PubMed: 17145498]
- Hanson MG, Landmesser LT. Characterization of the circuits that generate spontaneous episodes of activity in the early embryonic mouse spinal cord. *J Neurosci* 2003;23:587–600. [PubMed: 12533619]
- Hellstrom J. PhD Thesis. Karolinska Institute; Stockholm, Sweden: 2004. On the cholinergic C-bouton.
- Hellstrom J, Arvidsson U, Elde R, Cullheim S, Meister B. Differential expression of nerve terminal protein isoforms in VAcHT-containing varicosities of the spinal cord ventral horn. *J Comp Neurol* 1999;411:578–590. [PubMed: 10421869]
- Hellstrom J, Oliveira AL, Meister B, Cullheim S. Large cholinergic nerve terminals on subsets of motoneurons and their relation to muscarinic receptor type 2. *J Comp Neurol* 2003;460:476–486. [PubMed: 12717708]
- Herrero JL, Roberts MJ, Delicato LS, Gieselmann MA, Dayan P, Thiele A. Acetylcholine contributes through muscarinic receptors to attentional modulation in V1. *Nature* 2008;454:1110–1114. [PubMed: 18633352]
- Hinckley CA, Hartley R, Wu L, Todd A, Ziskind-Conhaim L. Locomotor-like rhythms in a genetically distinct cluster of interneurons in the mammalian spinal cord. *J Neurophysiol* 2005;93:1439–1449. [PubMed: 15496486]
- Hippenmeyer S, Vrieseling E, Sigrist M, Portmann T, Laengle C, Ladle DR, Arber S. A developmental switch in the response of DRG neurons to ETS transcription factor signaling. *PLoS Biol* 2005;3:e159.
- Hochman S, Schmidt BJ. Whole cell recordings of lumbar motoneurons during locomotor-like activity in the in vitro neonatal rat spinal cord. *J Neurophysiol* 1998;79:743–752. [PubMed: 9463437]
- Huang A, Noga BR, Carr PA, Fedirchuk B, Jordan LM. Spinal cholinergic neurons activated during locomotion: localization and electrophysiological characterization. *J Neurophysiol* 2000;83:3537–3547. [PubMed: 10848569]
- Hutchison DL, Roy RR, Hodgson JA, Edgerton VR. EMG amplitude relationships between the rat soleus and medial gastrocnemius during various motor tasks. *Brain Res* 1989;502:233–244. [PubMed: 2819462]
- Jankowska E. Spinal interneuronal systems: identification, multifunctional character and reconfigurations in mammals. *J Physiol* 2001;533:31–40. [PubMed: 11351010]
- Jessell TM. Neuronal specification in the spinal cord: inductive signals and transcriptional codes. *Nat Rev Genet* 2000;1:20–29. [PubMed: 11262869]
- Jiang Z, Carlin KP, Brownstone RM. An in vitro functionally mature mouse spinal cord preparation for the study of spinal motor networks. *Brain Res* 1999;816:493–499. [PubMed: 9878874]
- Jordan LM, Liu J, Hedlund PB, Akay T, Pearson KG. Descending command systems for the initiation of locomotion in mammals. *Brain Res Rev* 2008;57:183–191. [PubMed: 17928060]
- Joshua M, Adler A, Mitelman R, Vaadia E, Bergman H. Midbrain dopaminergic neurons and striatal cholinergic interneurons encode the difference between reward and aversive events at different epochs of probabilistic classical conditioning trials. *J Neurosci* 2008;28:11673–11684. [PubMed: 18987203]
- Katz PS. Intrinsic and extrinsic neuromodulation of motor circuits. *Curr Opin Neurobiol* 1995;5:799–808. [PubMed: 8805409]
- Kjaerulff O, Kiehn O. Distribution of networks generating and coordinating locomotor activity in the neonatal rat spinal cord in vitro: a lesion study. *J Neurosci* 1996;16:5777–5794. [PubMed: 8795632]

- Krieger P, Grillner S, El Manira A. Endogenous activation of metabotropic glutamate receptors contributes to burst frequency regulation in the lamprey locomotor network. *Eur J Neurosci* 1998;10:3333–3342. [PubMed: 9824446]
- Kwan AC, Dietz SB, Webb WW, Harris-Warrick RM. Activity of Hb9 interneurons during fictive locomotion in mouse spinal cord. *J Neurosci* 2009;29:11601–11613. [PubMed: 19759307]
- Lagerback PA, Ronnevi LO, Cullheim S, Kellerth JO. An ultrastructural study of the synaptic contacts of alpha-motoneurone axon collaterals. I. Contacts in lamina IX and with identified alpha-motoneurone dendrites in lamina VII. *Brain Res* 1981;207:247–266. [PubMed: 7470908]
- Lanuza GM, Gosgnach S, Pierani A, Jessell TM, Goulding M. Genetic identification of spinal interneurons that coordinate left-right locomotor activity necessary for walking movements. *Neuron* 2004;42:375–386. [PubMed: 15134635]
- Lawrence JJ. Cholinergic control of GABA release: emerging parallels between neocortex and hippocampus. *Trends Neurosci* 2008;31:317–327. [PubMed: 18556072]
- Li W, Ochalski PA, Brimijoin S, Jordan LM, Nagy JI. C-terminals on motoneurons: electron microscope localization of cholinergic markers in adult rats and antibody-induced depletion in neonates. *Neuroscience* 1995;65:879–891. [PubMed: 7609885]
- Li YW, Bayliss DA. Electrophysical properties, synaptic transmission and neuromodulation in serotonergic caudal raphe neurons. *Clin Exp Pharmacol Physiol* 1998;25:468–473. [PubMed: 9673827]
- Liu J, Akay T, Hedlund PB, Pearson KG, Jordan LM. Spinal 5-HT7 Receptors Are Critical for Alternating Activity During Locomotion: In Vitro Neonatal and In Vivo Adult Studies Using 5-HT7 Receptor Knockout Mice. *J Neurophysiol* 2009;102:337–348. [PubMed: 19458153]
- Liu W, Selever J, Lu MF, Martin JF. Genetic dissection of Pitx2 in craniofacial development uncovers new functions in branchial arch morphogenesis, late aspects of tooth morphogenesis and cell migration. *Development* 2003;130:6375–6385. [PubMed: 14623826]
- Lundfald L, Restrepo CE, Butt SJ, Peng CY, Droho S, Endo T, Zeilhofer HU, Sharma K, Kiehn O. Phenotype of V2-derived interneurons and their relationship to the axon guidance molecule EphA4 in the developing mouse spinal cord. *Eur J Neurosci* 2007;26:2989–3002. [PubMed: 18028107]
- Machacek DW, Hochman S. Noradrenaline unmasks novel self-reinforcing motor circuits within the mammalian spinal cord. *J Neurosci* 2006;26:5920–5928. [PubMed: 16738234]
- Maskos U, Molles BE, Pons S, Besson M, Guiard BP, Guilloux JP, Evrard A, Cazala P, Cormier A, Mamei-Engvall M, et al. Nicotine reinforcement and cognition restored by targeted expression of nicotinic receptors. *Nature* 2005;436:103–107. [PubMed: 16001069]
- Masuko S, Nakajima Y, Nakajima S, Yamaguchi K. Noradrenergic neurons from the locus ceruleus in dissociated cell culture: culture methods, morphology, and electrophysiology. *J Neurosci* 1986;6:3229–3241. [PubMed: 2430074]
- McCrea DA, Rybak IA. Organization of mammalian locomotor rhythm and pattern generation. *Brain Res Rev* 2008;57:134–146. [PubMed: 17936363]
- McHanwell S, Biscoe TJ. The localization of motoneurons supplying the hindlimb muscles of the mouse. *Philos Trans R Soc Lond B Biol Sci* 1981;293:477–508. [PubMed: 6115428]
- McLaughlin BJ. Propriospinal and supraspinal projections to the motor nuclei in the cat spinal cord. *J Comp Neurol* 1972;144:475–500.
- Mena-Segovia J, Winn P, Bolam JP. Cholinergic modulation of midbrain dopaminergic systems. *Brain Res Rev* 2008;58:265–271. [PubMed: 18343506]
- Miles GB, Hartley R, Todd AJ, Brownstone RM. Spinal cholinergic interneurons regulate the excitability of motoneurons during locomotion. *Proc Natl Acad Sci USA* 2007;104:2448–2453. [PubMed: 17287343]
- Misgeld T, Burgess RW, Lewis RM, Cunningham JM, Lichtman JW, Sanes JR. Roles of neurotransmitter in synapse formation: development of neuromuscular junctions lacking choline acetyltransferase. *Neuron* 2002;36:635–648. [PubMed: 12441053]
- Mizuguchi R, Kriks S, Cordes R, Gossler A, Ma Q, Goulding M. *Ascl1* and *Gsh1/2* control inhibitory and excitatory cell fate in spinal sensory interneurons. *Nat Neurosci* 2006;9:770–778. [PubMed: 16715081]

- Moran-Rivard L, Kagawa T, Saueressig H, Gross MK, Burrill J, Goulding M. Evx1 is a postmitotic determinant of v0 interneuron identity in the spinal cord. *Neuron* 2001;29:385–399. [PubMed: 11239430]
- Muennich EA, Fyffe RE. Focal aggregation of voltage-gated, Kv2.1 subunit-containing, potassium channels at synaptic sites in rat spinal motoneurons. *J Physiol* 2004;554:673–685. [PubMed: 14608003]
- Myers CP, Lewcock JW, Hanson MG, Gosgnach S, Aimone JB, Gage FH, Lee KF, Landmesser LT, Pfaff SL. Cholinergic input is required during embryonic development to mediate proper assembly of spinal locomotor circuits. *Neuron* 2005;46:37–49. [PubMed: 15820692]
- Nagy JI, Yamamoto T, Jordan LM. Evidence for the cholinergic nature of C-terminals associated with subsurface cisterns in alpha-motoneurons of rat. *Synapse* 1993;15:17–32. [PubMed: 8310422]
- Nicholson LF, Ma L, Goulding M. Cloning and expression of Munc 30: a member of the paired-like homeodomain gene family. *Cell Biol Int* 2001;25:351–365. [PubMed: 11319841]
- Orsal D, Perret C, Cabelguen JM. Evidence of rhythmic inhibitory synaptic influences in hindlimb motoneurons during fictive locomotion in the thalamic cat. *Exp Brain Res* 1986;64:217–224. [PubMed: 3021506]
- Pauli WM, O'Reilly RC. Attentional control of associative learning--a possible role of the central cholinergic system. *Brain Res* 2008;1202:43–53. [PubMed: 17870060]
- Pearson KG, Acharya H, Fouad K. A new electrode configuration for recording electromyographic activity in behaving mice. *J Neurosci Methods* 2005;148:36–42. [PubMed: 15908013]
- Peng CY, Yajima H, Burns CE, Zon LI, Sisodia SS, Pfaff SL, Sharma K. Notch and MAML signaling drives Scl-dependent interneuron diversity in the spinal cord. *Neuron* 2007;53:813–827. [PubMed: 17359917]
- Phelps PE, Barber RP, Houser CR, Crawford GD, Salvaterra PM, Vaughn JE. Postnatal development of neurons containing choline acetyltransferase in rat spinal cord: an immunocytochemical study. *J Comp Neurol* 1984;229:347–361. [PubMed: 6389614]
- Pierani A, Moran-Rivard L, Sunshine MJ, Littman DR, Goulding M, Jessell TM. Control of interneuron fate in the developing spinal cord by the progenitor homeodomain protein Dbx1. *Neuron* 2001;29:367–384. [PubMed: 11239429]
- Polgar E, Thomson S, Maxwell DJ, Al-Khater K, Todd AJ. A population of large neurons in laminae III and IV of the rat spinal cord that have long dorsal dendrites and lack the neurokinin 1 receptor. *Eur J Neurosci* 2007;26:1587–1598. [PubMed: 17880393]
- Quinlan KA, Placas PG, Buchanan JT. Cholinergic modulation of the locomotor network in the lamprey spinal cord. *J Neurophysiol* 2004;92:1536–48. [PubMed: 15152024]
- Roberts A, Li WC, Soffe SR, Wolf E. Origin of excitatory drive to a spinal locomotor network. *Brain Res Rev* 2008;57:22–28. [PubMed: 17825424]
- Roy RR, Hirota WK, Kuehl M, Edgerton VR. Recruitment patterns in the rat hindlimb muscle during swimming. *Brain Res* 1985;337:175–178. [PubMed: 4005606]
- Sapir T, Geiman EJ, Wang Z, Velasquez T, Mitsui S, Yoshihara Y, Frank E, Alvarez FJ, Goulding M. Pax6 and engrailed 1 regulate two distinct aspects of rensaw cell development. *J Neurosci* 2004;24:1255–1264. [PubMed: 14762144]
- Semina EV, Reiter R, Leysens NJ, Alward WL, Small KW, Datson NA, Siegel-Bartelt J, Bierke-Nelson D, Bitoun P, Zabel BU, et al. Cloning and characterization of a novel bicoid-related homeobox transcription factor gene, RIEG, involved in Rieger syndrome. *Nat Genet* 1996;14:392–399. [PubMed: 8944018]
- Shefchyk SJ, Jordan LM. Motoneuron input-resistance changes during fictive locomotion produced by stimulation of the mesencephalic locomotor region. *J Neurophysiol* 1985;54:1101–1108. [PubMed: 4078609]
- Smith BN, Banfield BW, Smeraski CA, Wilcox CL, Dudek FE, Enquist LW, Pickard GE. Pseudorabies virus expressing enhanced green fluorescent protein: A tool for in vitro electrophysiological analysis of transsynaptically labeled neurons in identified central nervous system circuits. *Proc Natl Acad Sci USA* 2000;97:9264–9269. [PubMed: 10922076]
- Stacy RC, Demas J, Burgess RW, Sanes JR, Wong RO. Disruption and recovery of patterned retinal activity in the absence of acetylcholine. *J Neurosci* 2005;25:9347–9357. [PubMed: 16221843]

- VanderHorst VG, Ulfhake B. The organization of the brainstem and spinal cord of the mouse: relationships between monoaminergic, cholinergic, and spinal projection systems. *J Chem Neuroanat* 2006;31:2–36. [PubMed: 16183250]
- Wang Z, Kai L, Day M, Ronesi J, Yin HH, Ding J, Tkatch T, Lovinger DM, Surmeier DJ. Dopaminergic control of corticostriatal long-term synaptic depression in medium spiny neurons is mediated by cholinergic interneurons. *Neuron* 2006;50:443–452. [PubMed: 16675398]
- Wess J. Novel insights into muscarinic acetylcholine receptor function using gene targeting technology. *Trends Pharmacol Sci* 2003;24:414–420. [PubMed: 12915051]
- Wichterle H, Lieberam I, Porter JA, Jessell TM. Directed differentiation of embryonic stem cells into motor neurons. *Cell* 2002;110:385–397. [PubMed: 12176325]
- Willis WD. The case for the Renshaw cell. *Brain Behav Evol* 1971;4:5–52. [PubMed: 4331276]
- Wilson JM, Hartley R, Maxwell DJ, Todd AJ, Lieberam I, Kaltschmidt JA, Yoshida Y, Jessell TM, Brownstone RM. Conditional rhythmicity of ventral spinal interneurons defined by expression of the Hb9 homeodomain protein. *J Neurosci* 2005;25:5710–5719. [PubMed: 15958737]
- Wilson JM, Rempel J, Brownstone RM. Postnatal development of cholinergic synapses on mouse spinal motoneurons. *J Comp Neurol* 2004;474:13–23. [PubMed: 15156576]
- Winkowski DE, Knudsen EI. Distinct mechanisms for top-down control of neural gain and sensitivity in the owl optic tectum. *Neuron* 2008;60:698–708. [PubMed: 19038225]

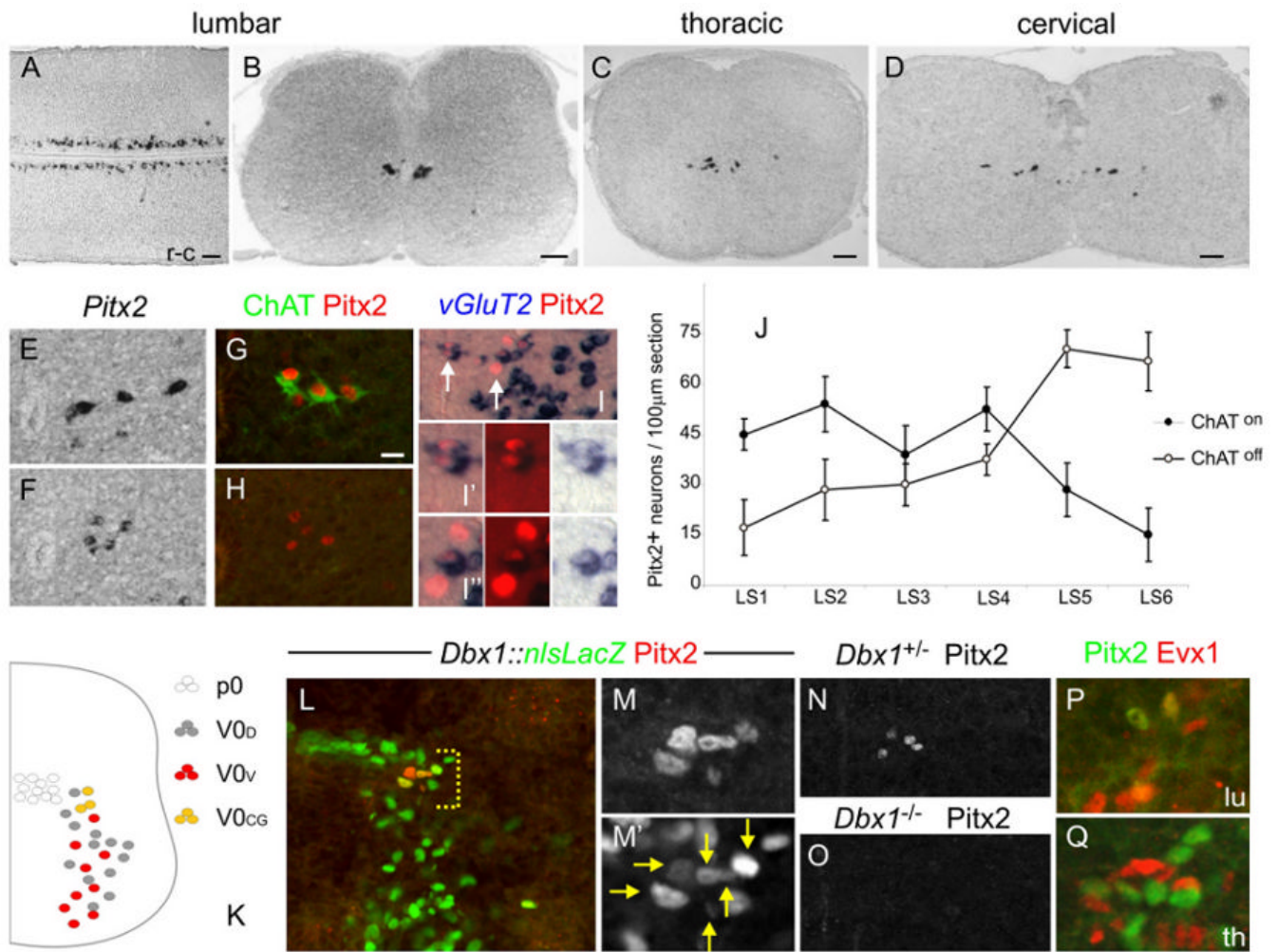


(Figure S7). These non-cholinergic neurons likely correspond to neurons described by Polgar et al. (2007).

Scale bars = 100 μ m (A-D), 20 μ m (G).

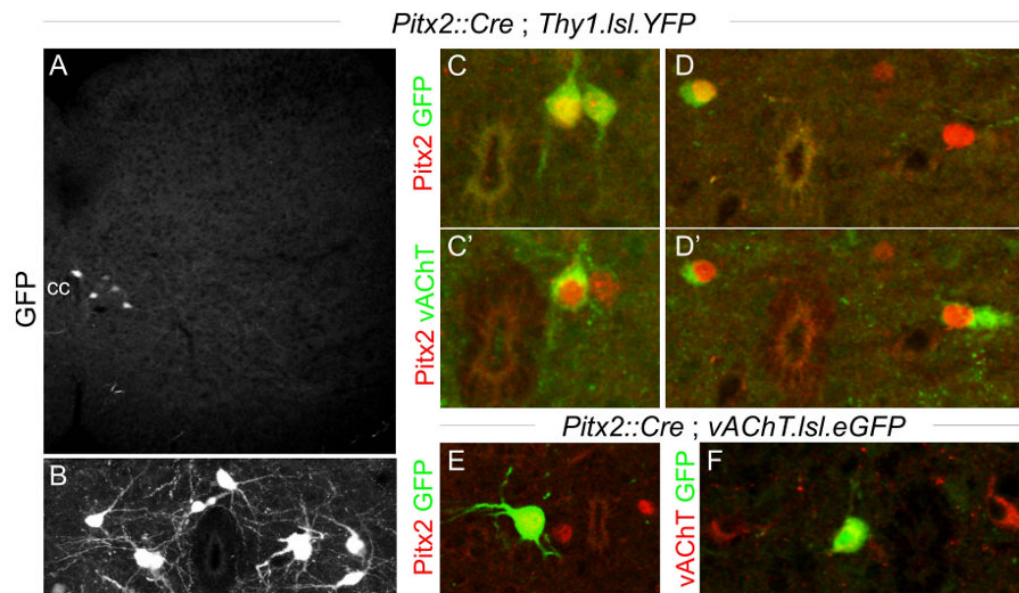


Figure 2. Genetic marking of $Pitx2^+$ neurons

(A-D') Genetic marking of $Pitx2^+$ neurons in *Pitx2::Cre; Thy1.lsl.YFP* mice.

(A, B) Fluorescent protein (FP) is expressed in a small subset of peri-central canal neurons (cc: central canal). B shows high power view of the peri-central canal region. (C, D) In this *Thy1* line, FP is expressed in 66% of $Pitx2^+$ neurons. (C', D') FP and vAChT expression at rostral lumbar levels.

(E, F) Genetic marking of $V0_C$ neurons in *Pitx2::Cre; vAChT.lsl.eGFP* mice reveals FP expression in $Pitx2^+$ and vAChT $^+$ neurons.

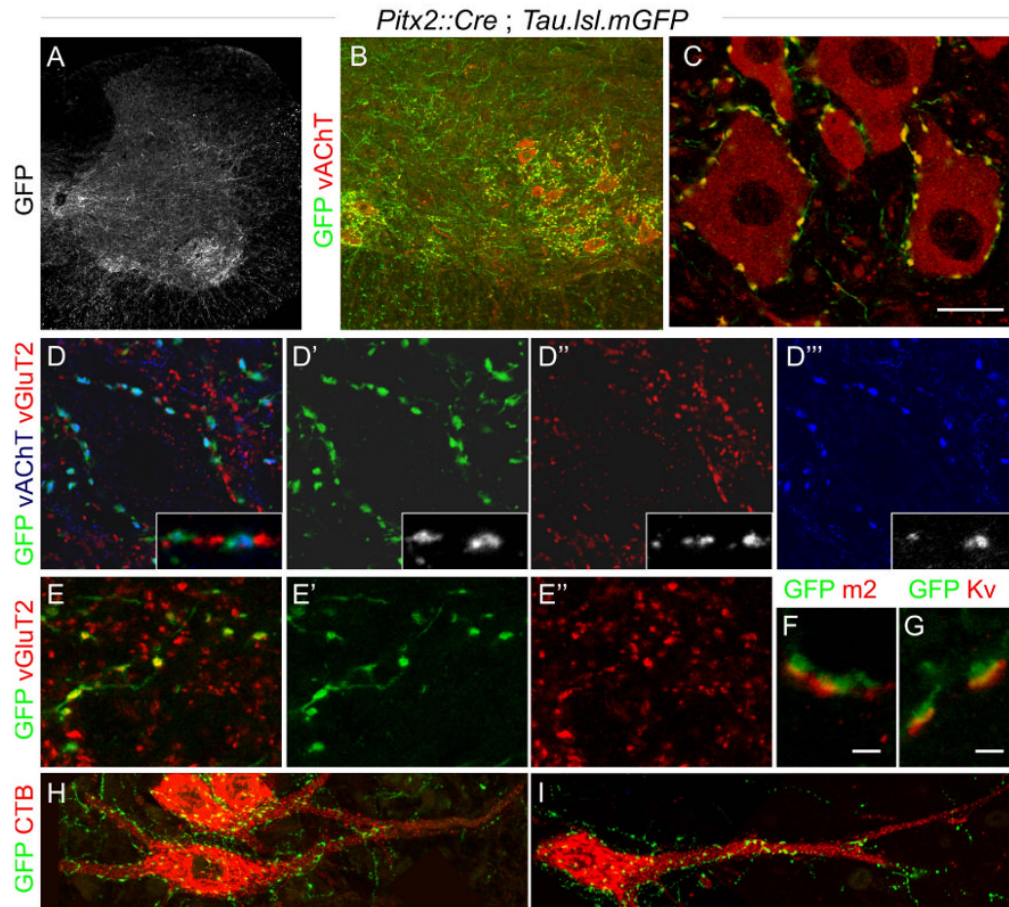


Figure 3. Genetic tracing of V0_C neuronal connections with motor neurons

(A) Spatial distribution of V0_C and V0_G axons and terminals in lumbar spinal cord of *Pitx2::Cre; Tau.lsl.mGFP* reporter mice.

(B, C) Co-expression of FP and vAChT in C-boutons. >95% of vAChT⁺ terminals on motor neurons express FP. The density of FP-labeled boutons on motor neurons that innervate proximal hindlimb muscles was ~3-fold greater than that on motor neurons innervating distal footpad (plantar) muscles, consistent with the known pattern of C-bouton innervation (Hellstrom, 2004).

(D-D''') FP⁺ terminals motor neurons express vAChT but not vGluT2.

(E-E''') FP⁺ terminals in the intermediate spinal cord express vGluT2.

(F, G) In *Pitx2::Cre; Tau.lsl.mGFP* mice, m2 muscarinic receptor (m2) and Kv2.1 channel (Kv) clusters are aligned with FP⁺ C-boutons.

(H, I) FP⁺ C-boutons are concentrated on motor neuron somata and proximal dendrites. Cholera toxin B (CTB) subunit-labeled tibialis anterior motor neurons in lumbar spinal cord of a p24 *Pitx2::Cre; Tau.lsl.mGFP* mouse. FP-labeled terminals are detected on the soma and proximal dendrites (15.7 C-boutons/50 micron length of proximal dendrite, n = 3), but more distal dendritic domains are devoid of FP⁺ terminals.

Scale bars = 20µm (C), 2µm (F, G).

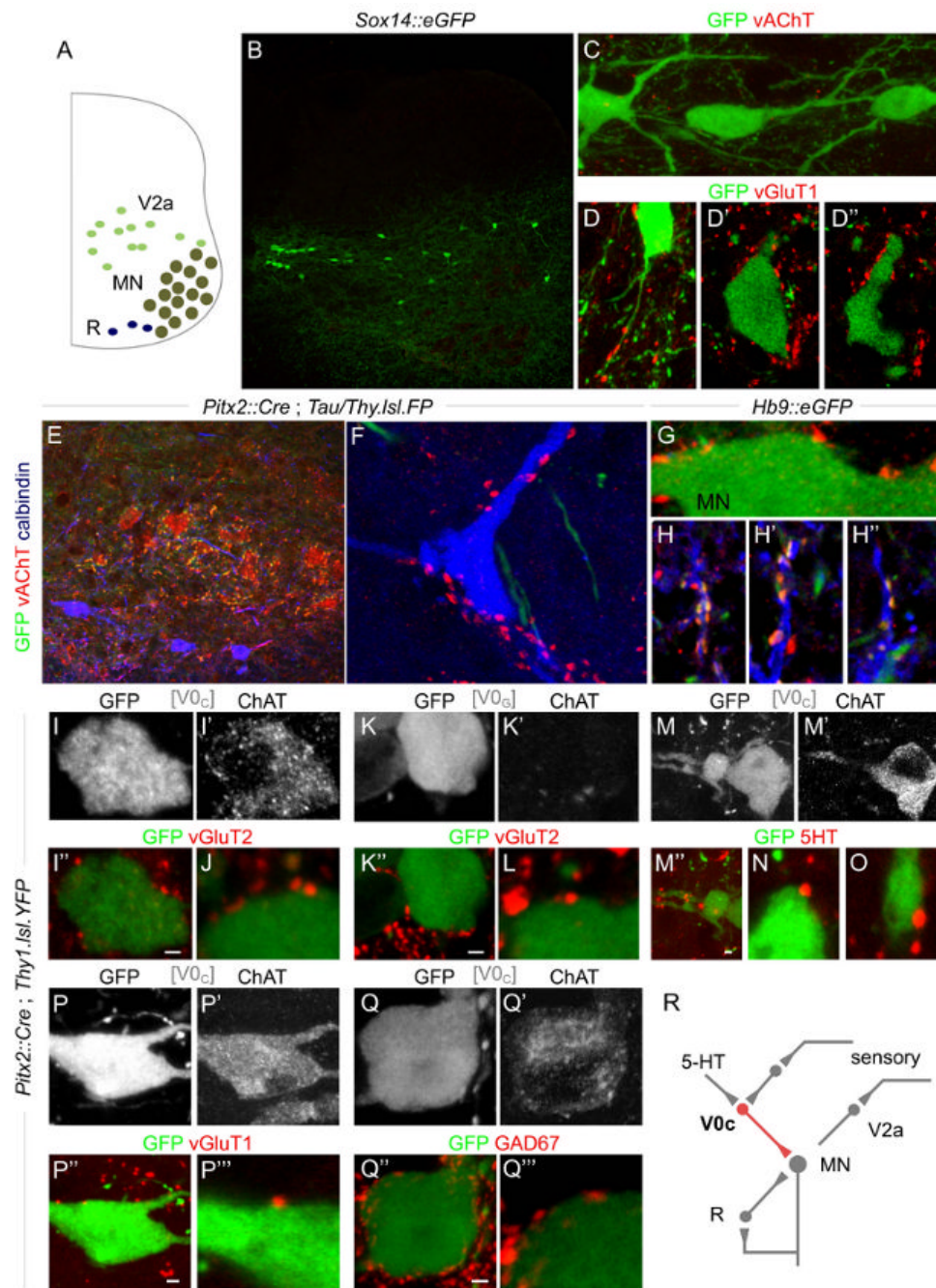


Figure 4. The synaptic circuitry of V0_C interneurons

(A-H'') Lack of connectivity of V0_C neurons with identified interneurons.

(A) Motor neuron (MN), Sox14⁺ V2a interneuron (V2a) and calbindin⁺ Renshaw cell (R) position in lumbar spinal cord.

(B) GFP⁺ V2a interneurons in lumbar spinal cord of p15 *Sox14::eGFP* mice.

(C) GFP labeled Sox14⁺ neurons are contacted by few vAChT⁺ terminals (<4 boutons per neuron, 37 neurons).

(D-D'') vGluT1⁺ terminals on dorsally located Sox14⁺ interneurons.

(E, F) In p24 *Pitx2cre; Tau/Thy1.lsl.FP* mice, calbindin⁺ Renshaw cells are contacted by vAChT terminals that do not express FP (n = 0/132 boutons, 8 neurons).

(G) GFP⁺ motor neurons in *Hb9::eGFP* mice lack FP⁺ vAChT input.
(H-H'') In p21 *Hb9::eGFP* mice, most vAChT⁺ terminals on calbindin⁺ Renshaw cells express FP.
(I-Q''') Synaptic inputs to p24 V0_{CG} interneurons.
(I-J) ChAT⁺, GFP⁺ V0_C neurons contacted by vGluT2⁺ boutons. Panel J shows a different neuron.
(K-L) ChAT^{off}, GFP⁺ V0_G neurons also contacted by vGluT2⁺ boutons. Panel L shows a different neuron.
(M-O) ChAT⁺, GFP⁺ V0_C neurons contacted by 5HT⁺ boutons. Panels N and O show different neurons.
(P-P''') ChAT⁺, GFP⁺ V0_C neurons contacted by vGluT1⁺ boutons.
(Q-Q''') ChAT⁺, GFP⁺ V0_C neurons contacted by GAD67⁺ boutons.
(R) Connectivity of V0_C neurons.
Scale bar = 2μm (I'', K'', M'', P'', Q'').

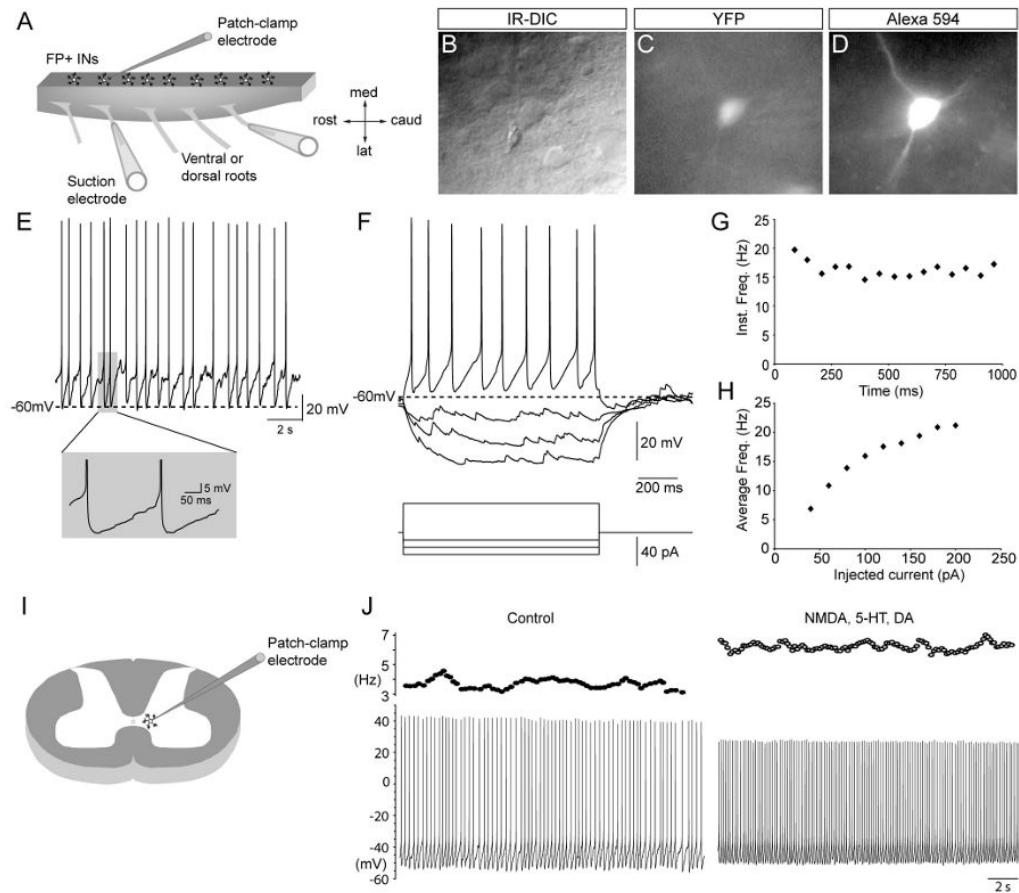


Figure 5. Intrinsic properties of $Pitx2^+$ $V0_{CG}$ interneurons

(A) Hemisectioned spinal cord preparation used for physiology.

(B-D) IR-DIC and fluorescence images of an identified $V0_{CG}$ neuron from a *Pitx2::Cre; Thy1.lsl.YFP* mouse. The cell was patch-clamped under IR-DIC optics and filled with Alexa 594 during recording.

(E) Slow frequency, tonic activity recorded from a FP-labeled $V0_{CG}$ neuron. Prominent after-hyperpolarization shown in grey inset.

(F) Recordings from a FP-labeled $V0_{CG}$ neuron after injection of depolarizing and hyperpolarizing current pulses (1s duration). Bottom trace shows injected current.

(G) Instantaneous firing frequency of a FP-labeled $V0_{CG}$ neuron in response to 1s injection of depolarizing current.

(H) Steady-state firing frequency - current plot ($f-I$) for a FP-labeled $V0_{CG}$ neuron upon injection of incremental (1s) depolarizing current steps.

(I) Spinal cord slice preparation.

(J) Instantaneous firing frequency (moving average of 5 consecutive spikes; top) and corresponding current-clamp recordings (bottom) from a tonically active *Thy1* FP-labeled $V0_{CG}$ neuron in a slice preparation. Control (left) and with NMDA ($5\mu\text{M}$), 5-HT ($10\mu\text{M}$) and dopamine ($50\mu\text{M}$) (right).

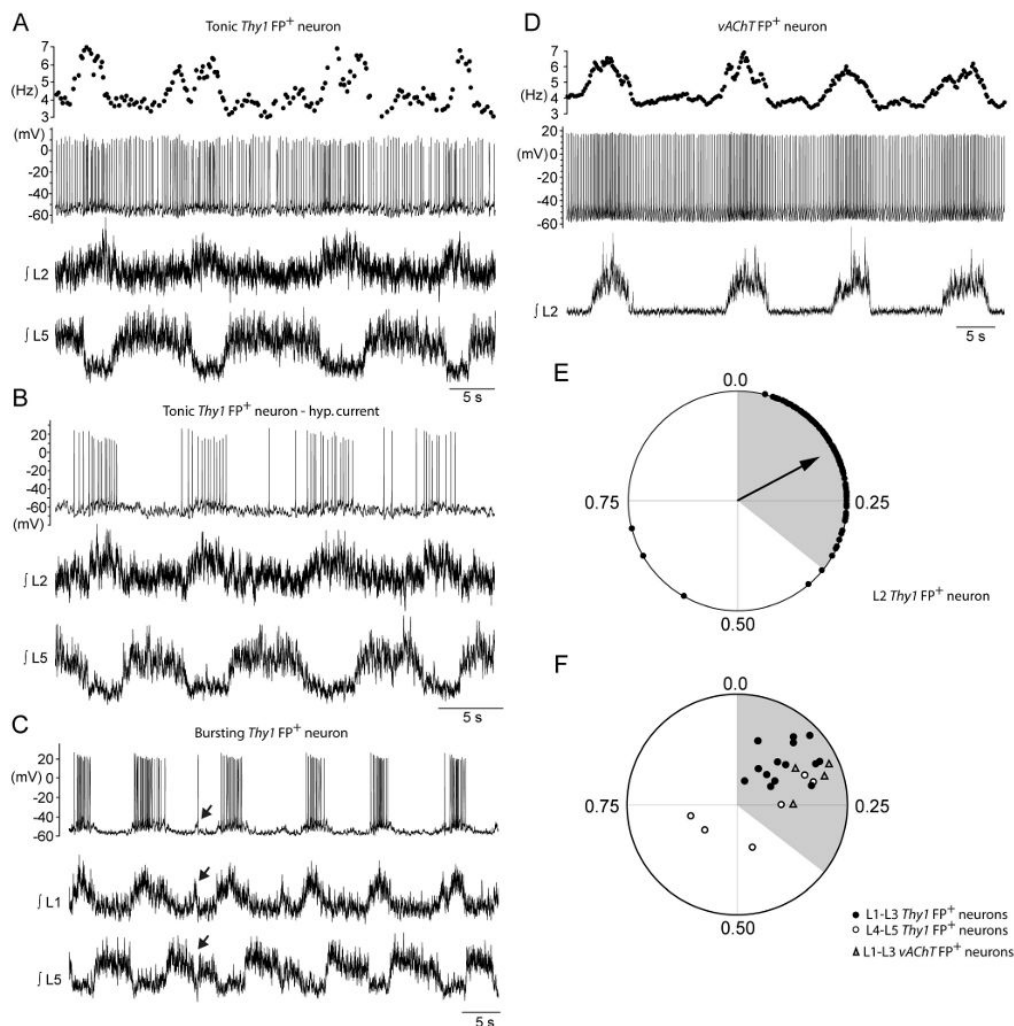


Figure 6. Activity of $Pitx2^+$ $V0_{CG}$ neurons during locomotor episodes

(A) Moving average (5 consecutive spikes) of the instantaneous firing frequency of a tonically active *Thy1* FP-labeled $V0_{CG}$ neuron (top trace) along with the corresponding current-clamp recording (2nd trace) and rectified/integrated ventral root recordings (bottom traces) during drug-induced (NMDA $5\mu\text{M}$, 5-HT $10\mu\text{M}$, dopamine $50\mu\text{M}$) locomotor activity in a hemisectioned spinal cord preparation.

(B) Phasic activity recorded from neuron in A during the injection of hyperpolarizing current (top trace) along with rectified/integrated recordings of locomotor activity from ventral roots (bottom traces).

(C) Recording from a bursting *Thy1* FP-labeled $V0_{CG}$ neuron (top trace) and rectified/integrated recordings of locomotor activity from ventral roots (bottom traces). The coupling between the spiking of this FP-labeled $V0_{CG}$ neuron and ventral root activity is indicated by arrows.

(D) Moving average (5 consecutive spikes) of the instantaneous firing frequency of a tonically active *vAChT* FP-labeled $V0_C$ neuron (top trace) along with the corresponding current-clamp recording (2nd trace) and rectified/integrated recordings of locomotor activity from ventral roots (bottom traces).

(E) Circular plot for the FP-labeled $V0_{CG}$ neuron shown in C depicting its preferred firing phase (mean vector; arrow) in relation to the locomotor cycle. The start of the locomotor cycle

(0.0) is taken as the onset of the burst in the rostral lumbar ventral root. Shaded area highlights the average duration of rostral lumbar root activity. Each point on the circle corresponds to a single action potential. The direction of the mean vector indicates the preferred firing phase of the neuron, and the length of the vector indicates the tuning of action potentials around their mean.

(F) Circular plot showing the preferred firing phases (position of mean vectors) for all FP-labeled $V0_{CG}$ neurons, revealing a significant correlation with ventral root bursting (Rayleigh test, $p < 0.05$). Data include neurons from *Pitx2::Cre; Thy1.lsl.YFP* (L1-L3 levels, closed circles; L4-L5 levels, open circles) and *Pitx2::Cre; vAChT* mice (L1-L3 levels, open triangles).

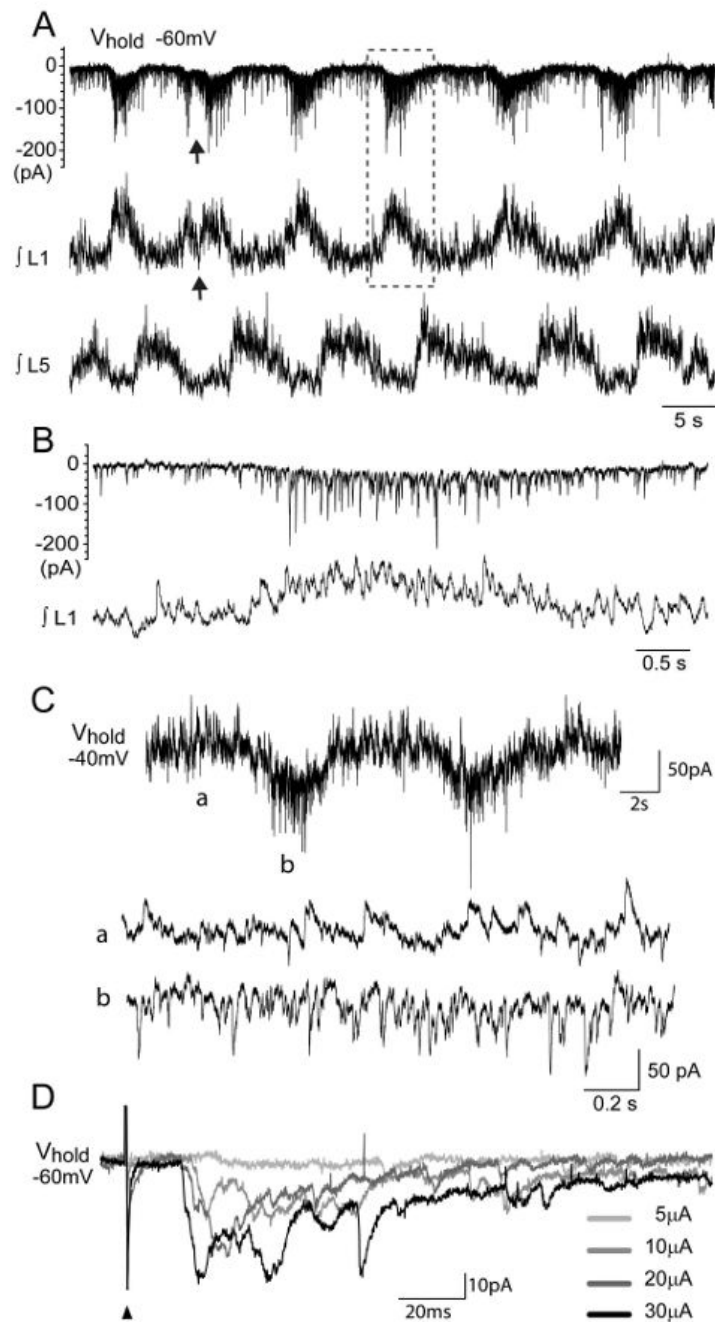


Figure 7. Synaptic inputs to $Pitx2^+$ $V0_{CG}$ interneurons

(A) Voltage-clamp recording of a *Thy1* FP-labeled $V0_{CG}$ neuron held at $-60mV$ (top trace) and rectified/integrated ventral root recordings (bottom traces) during drug-induced (NMDA $5\mu M$, 5-HT $10\mu M$, dopamine $50\mu M$) locomotor activity in a hemisected spinal cord preparation. The coupling between EPSCs recorded in this FP-labeled $V0_{CG}$ neuron and L1 ventral root activity is indicated by arrows.

(B) A volley of EPSCs recorded from the FP-labeled $V0_{CG}$ neuron in A (top trace) and a simultaneous ventral root burst (bottom trace). These data are outlined by the dotted box in A.

(C) Voltage-clamp recordings of a *Thy1* FP-labeled $V0_{CG}$ neuron held at -40mV reveal IPSCs throughout the locomotor cycle. Bottom two traces show data from the time points marked 'a' and 'b' in the top trace.

(D) Voltage-clamp recording of EPSCs evoked in a *Thy1* FP-labeled $V0_{CG}$ neuron by dorsal root stimulation (5-30 μ A, 0.5 ms). Each trace is an average of 5 sweeps, arrowhead points to stimulus artefact).

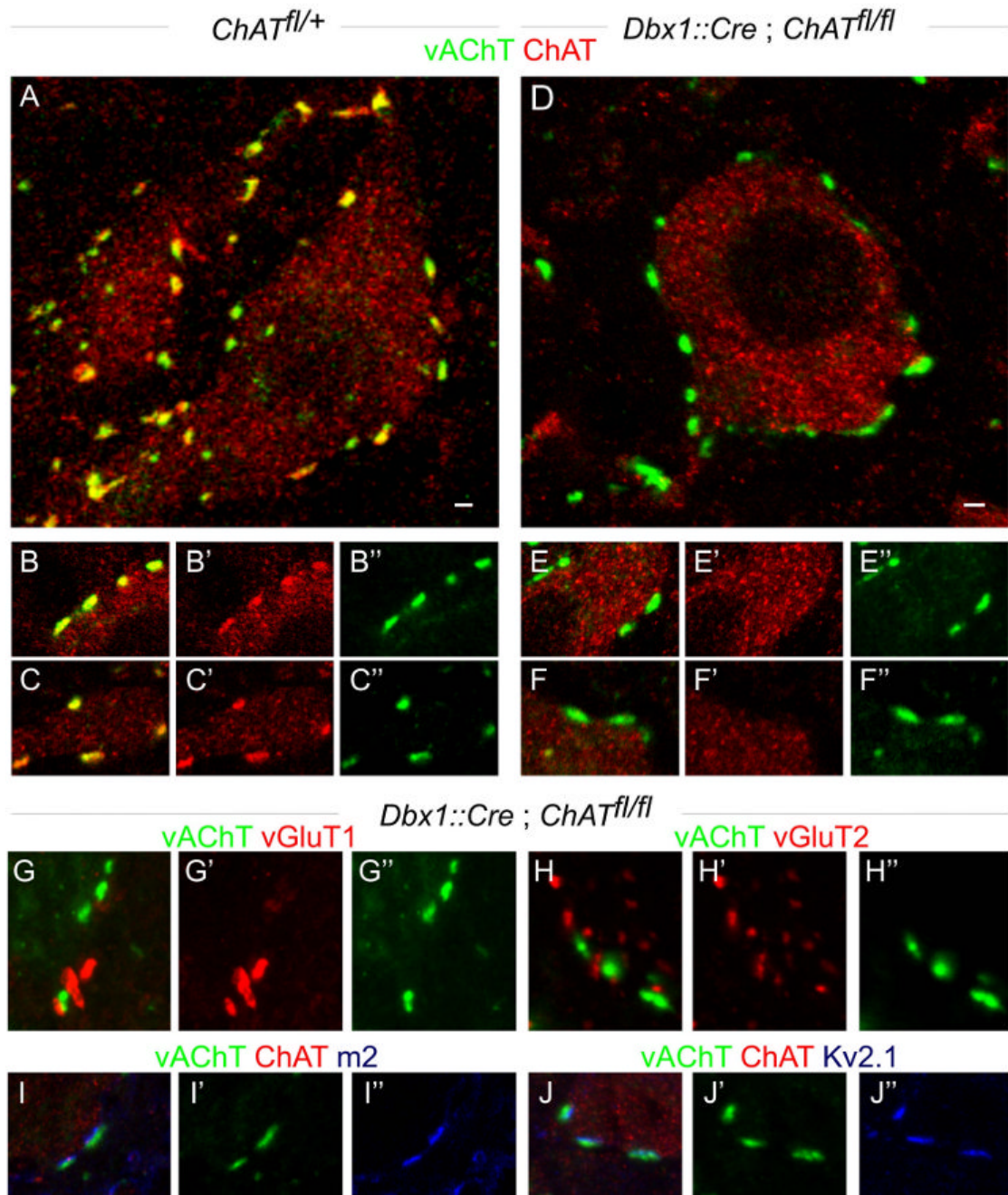


Figure 8. Genetically programmed elimination of ChAT from V0C interneurons

(A-C'') Lumbar motor neurons in p24 *ChAT^{fl/+}* mice express ChAT. C-bouton terminals on motor neurons express both vAChT and ChAT.

(D-F'') Lumbar motor neurons in p24 *Dbx1::cre; ChAT^{fl/fl}* mice express ChAT. Their C-bouton inputs express vAChT, but not ChAT (n = 503 boutons from 2 p24 and 3 p60 mice).

(G-H'') In *Dbx1::cre; ChAT^{fl/fl}* mice (p24 and p60), ChAT depleted C-boutons do not express vGluT1 (G) or vGluT2 (H).

(I-J'') In *Dbx1::cre; ChAT^{fl/fl}* mice (p60), m2 muscarinic receptors (I) and Kv2.1 channels (J) are clustered in alignment with vAChT⁺, ChAT-deficient C-boutons.

Scale bar = 2 μ m (A, D).

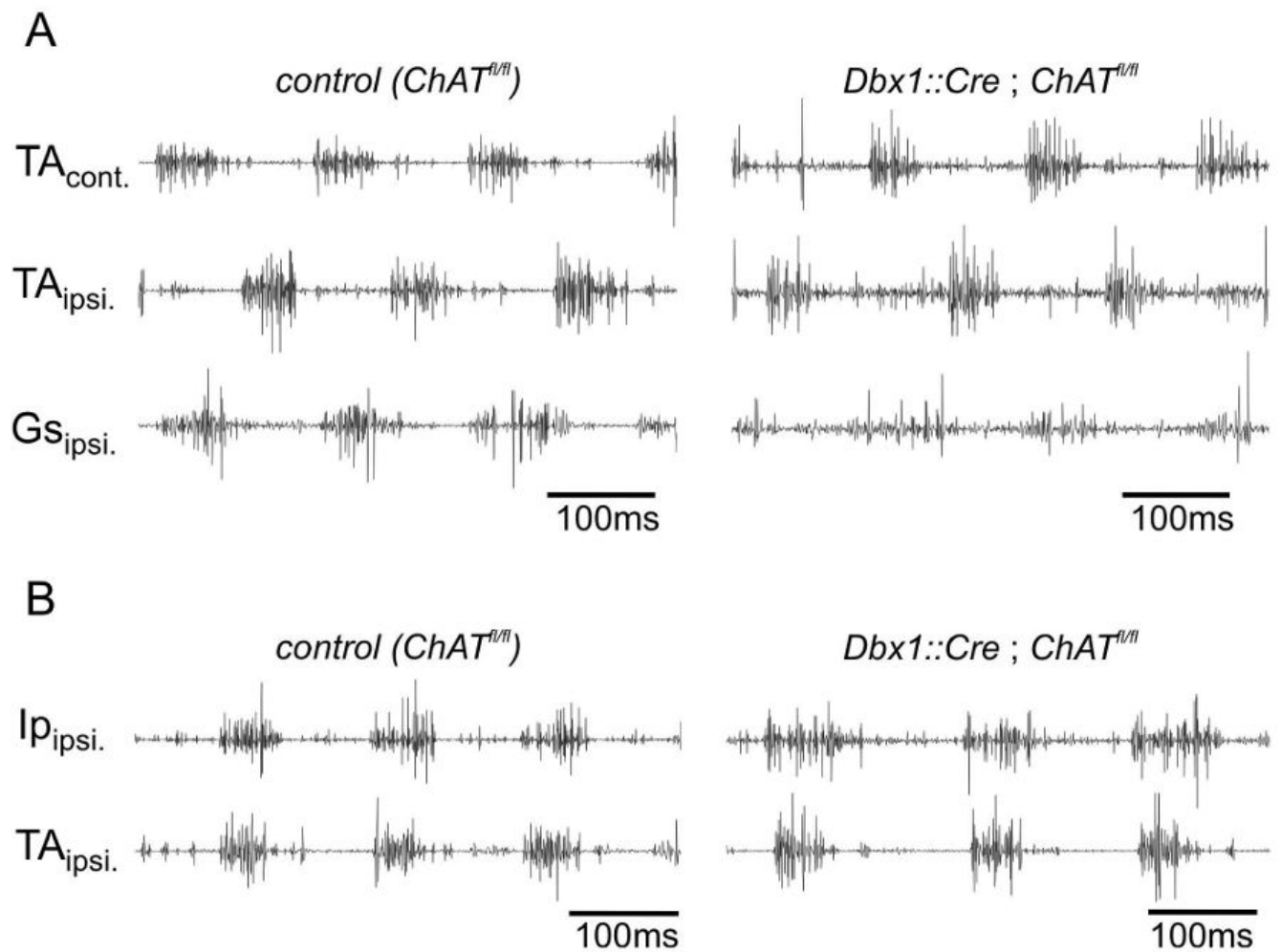


Figure 9. Preservation of basic locomotor pattern in mice with ChAT-depleted V0_C neurons
 (A) EMG recordings from the contralateral tibialis anterior (TA_{cont.}, ankle flexor), ipsilateral TA (TA_{ipsi.}) and the ipsilateral gastrocnemius (Gs_{ipsi.}, ankle extensor) in control (*Chat^{fl/fl}*, left recordings; n = 7) and ChAT-depleted V0_C neuron mice (*Dbx1::Cre; Chat^{fl/fl}*) (right recordings; n = 8 mice), during walking.

(B) In-phase activation of flexor muscles acting on different joints of the same leg (iliopsoas, Ip_{ipsi.}, hip flexor and TA_{ipsi.}, ankle flexor) is preserved in control (*Chat^{fl/fl}*) (left recordings; n = 5) and ChAT-depleted V0_C neuron mice (*Dbx1::Cre; Chat^{fl/fl}*) (right recordings; n = 4), during walking.

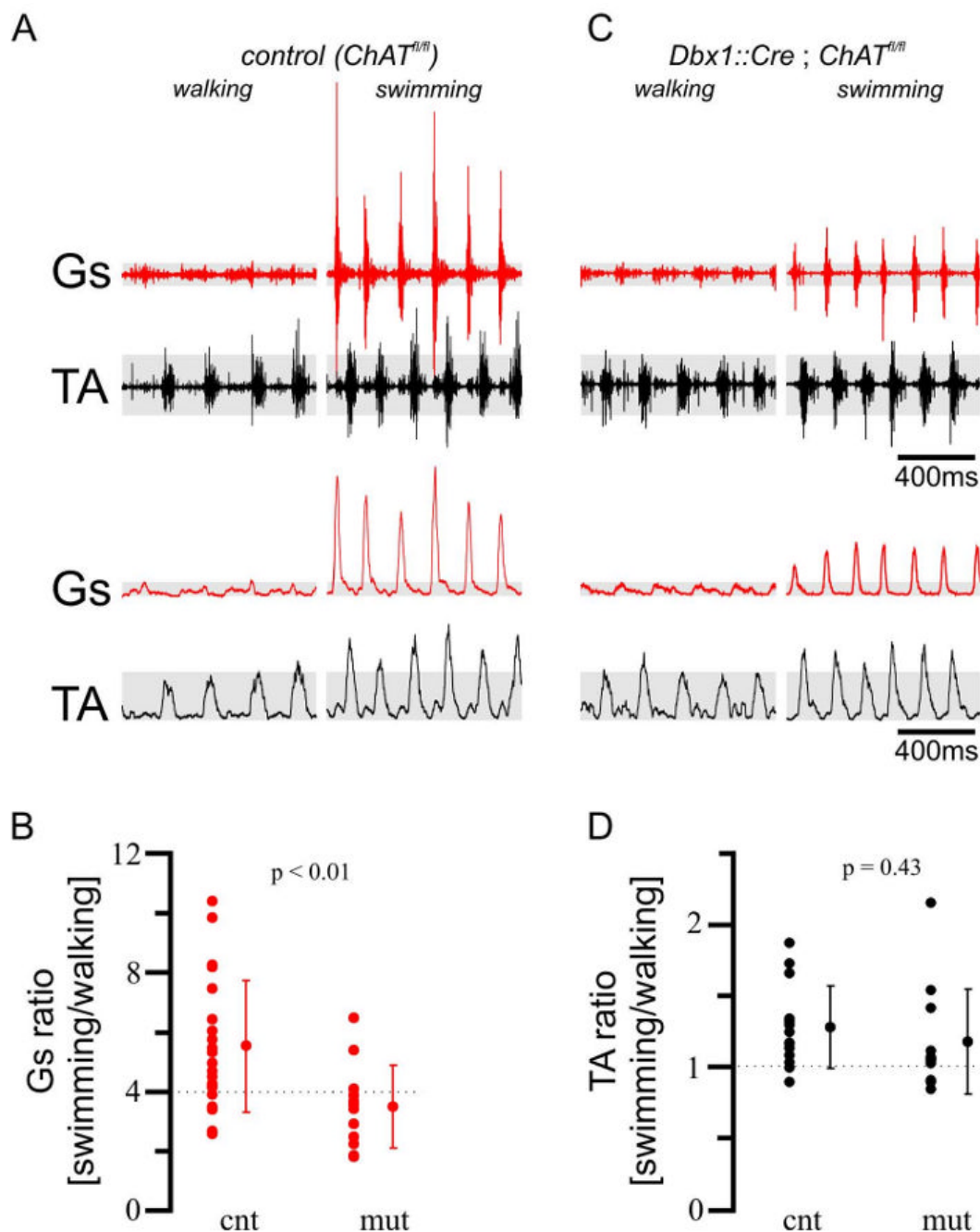


Figure 10. Task-specific impairment in gastrocnemius muscle activation in mice with ChAT-depleted V0_C neurons

(A) EMG recordings from Gs (red) and TA (black) muscles during walking (left) and swimming (right), in control (*Chat^{fl/fl}*) mice. Raw and integrated EMG traces are shown. (B) Ratio of Gs EMG amplitudes during walking and swimming in control wt (n = 8) and *Chat^{fl/fl}* (n = 14 mice) and from V0_C ChAT-deficient *Dbx1::Cre; Chat^{fl/fl}* mice (n = 12 mice). The Gs data obtained from wt and *Chat^{fl/fl}* mice were pooled, since they were not statistically different (p=0.13). The ratio of average peak values of Gs EMG activities during swimming and walking was significantly lower for *Dbx1::Cre; Chat^{fl/fl}* mice compared to controls. (C) EMG recordings from Gs (red) and TA (black) muscles during walking (left) and swimming (right), in *Dbx1::Cre; Chat^{fl/fl}* mice. Raw and integrated EMG traces are shown. (D) Ratio of TA EMG amplitudes during walking and swimming in control wt (n = 8) and *Chat^{fl/fl}* (n = 14 mice) and from V0_C ChAT-deficient *Dbx1::Cre; Chat^{fl/fl}* mice (n = 12 mice). The TA data obtained from wt and *Chat^{fl/fl}* mice were pooled, since they were not statistically different (p=0.43). The ratio of average peak values of TA EMG activities during swimming and walking was not significantly different for *Dbx1::Cre; Chat^{fl/fl}* mice compared to controls.

(C) EMG recordings from Gs (red) and TA (black) muscles during walking (left) and swimming (right), in *Dbx1::Cre; Chat^{fl/fl}* mice.

(D) Ratio of TA EMG amplitudes during walking and swimming in control *Chat^{fl/fl}* (n = 12) and V0_C ChAT-deficient *Dbx1::Cre; Chat^{fl/fl}* mice (n = 14 mice).

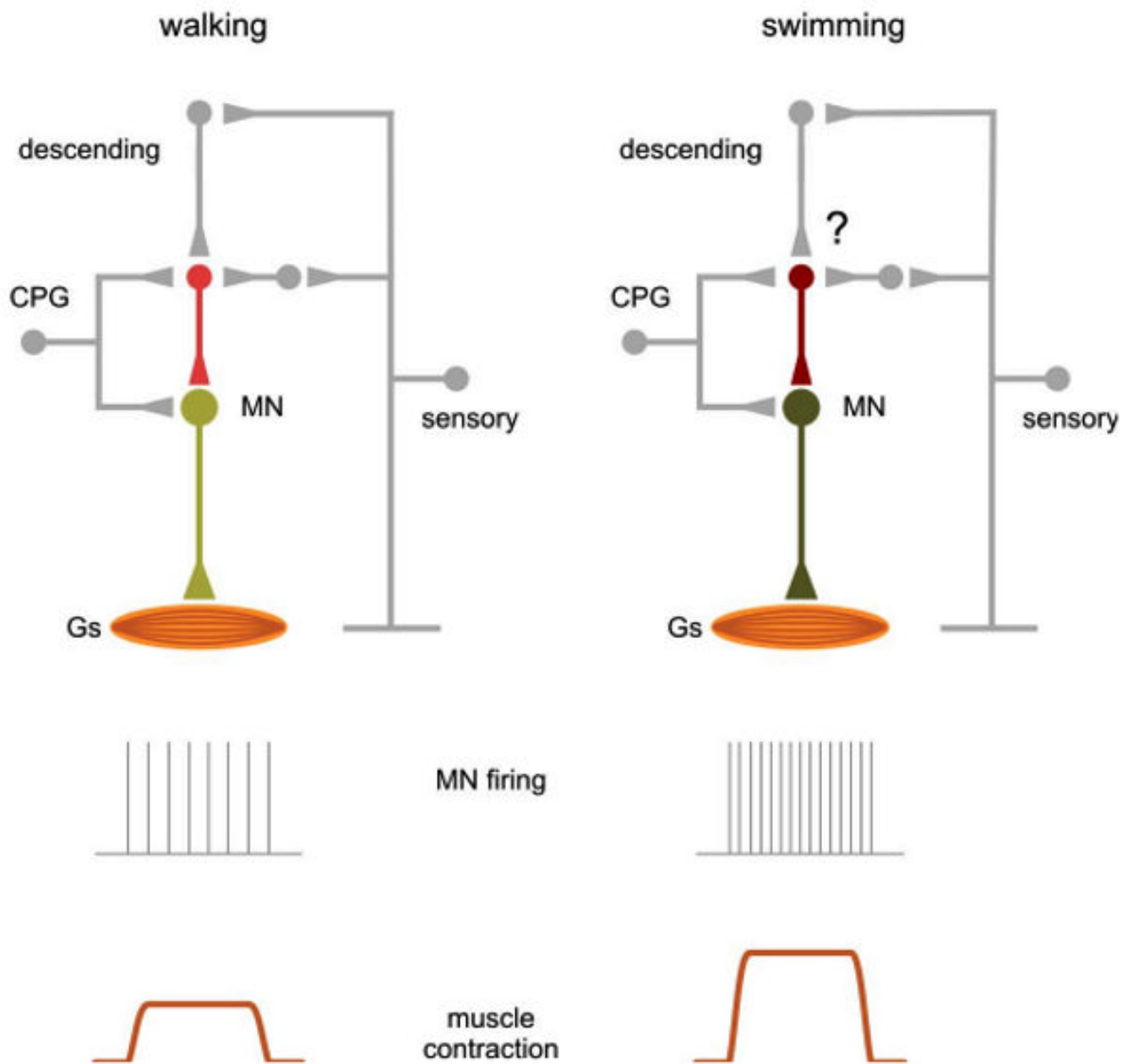


Figure 11. Intrinsic Neuromodulatory Role of $V0_C$ interneurons

A model of the intraspinal circuitry and function of $Pitx2^+$ $V0_C$ interneurons. $V0_C$ neurons form numerous cholinergic C-bouton synaptic contacts with motor neurons. They receive direct synaptic input from excitatory interneurons involved in the rhythmogenic central pattern generator (CPG) system, inputs from descending pathways, and indirect input from sensory afferents. During walking, the combined influence of these synaptic inputs results in a moderate level activation of the set of $V0_C$ neurons that innervate Gs motor neurons, which together with direct CPG input to motor neurons, results in an intermediate rate of Gs motor neuron firing and a modest contraction of the Gs muscle. During swimming, a task-dependent change in the activity of sensory and descending pathways increases the level of activation of $V0_C$ neurons, activating muscarinic m2 receptors on motor neurons, enhancing Gs motor neuron firing

frequency (Miles et al., 2007), and increasing the amplitude of Gs muscle contraction. For simplicity, we have not depicted direct descending modulatory inputs to motor neurons, which could contribute to the task-dependent modulation of Gs motor neuron activity. The question mark indicates the uncertain nature of the descending and/or sensory inputs that mediate the task-dependent regulation of $V0_C$ neuronal activity.